RIVM report 728001026/2003

Multi-gas emission profiles for stabilising greenhouse gas concentrations
Emission implications of limiting global temperature increase to 2°C

B. Eickhout, M.G.J. den Elzen and
D.P. van Vuuren

Abstract

In this report we present two CO_2-equivalent emission profiles leading to two different stabilised greenhouse gas concentration levels. The contribution of the various greenhouse gas emissions is expressed in CO_2-equivalent emissions. These equivalent emissions are determined by using the concept of Global Warming Potential (GWP). Moreover the radiative forcing of the emission profiles are summed resulting in CO_2 equivalent concentration levels. The profile leading to 550 ppmv CO_2-equivalents can result in a maximum global mean temperature increase of less than 2°C above pre-industrial level (i.e. 1765), with a low to medium value for climate sensitivity. The profile leading to 650 ppmv CO_2-equivalents only remains below the 2°C level if the value for climate sensitivity is at the low end of the range, which means that this profile is unlikely to meet the 2°C target. With a high climate sensitivity of 4.5°C, the target will not be met under either profile. A robust conclusion is that the 550 ppmv CO_2-equivalent stabilisation level can only be reached if global emissions peak around 2015 or if an overshoot of 550 ppmv is allowed. Other conclusions also depend on the level of sulphur emission reductions and the share of non-CO_2 greenhouse gas emissions in the reductions. Sulphur emissions are not taken into account in the GWP concept, but only have a small effect on the temperature increase in the short term. In the default analyses it is assumed that non-CO_2 greenhouse gases contribute 100 ppmv CO_2-equivalents in both profiles. From a sensitivity analysis we concluded that the variation in the contribution of non-CO_2 greenhouse gas emissions leads to a variation of $\pm$ 50 ppmv in CO_2-equivalents and $\pm$ 0.2°C temperature change in the short term (i.e. until 2100). This effect occurs since the GWP concept tends to underestimate the effect of efforts to reduce the emissions of short-lived gases such as CH_4. The effects of CO_2 mitigation measures are underestimated in the long-term (over 100 years). This shows that the validity of the GWP concept beyond short-term emission goals is limited.

Acknowledgements

Contents

Samenvatting

In dit rapport presenteren we twee broeikasgas emissieprofielen die leiden tot twee verschillende stabilisatieniveaus van concentraties. De multi-gas emissieprofielen zijn gebaseerd op het 'Global Warming Potential' (GWP) concept. De concentratieniveaus zijn berekend aan de hand van de som van de stralingsforcering van de Kyoto gassen (CO_2, CH_4, N_2O en de F-gassen). Het profiel dat stabiliseert op 550 ppmv CO_2-equivalenten resulteert in een temperatuurtoename tot onder de 2°C wanneer de klimaatgevoeligheid wordt gevarieerd tussen de 1.5°C en 2.5°C. Bij hogere waardes van de klimaatgevoeligheid zal het profiel leiden tot hogere temperatuurtoenames, daarmee het EU-doel overschrijdend. De onzekerheidsband van de klimaatgevoeligheid is gesteld op 1.5°C tot 4.5°C. Verder blijkt dat het 2°C doel bij het 650 ppmv stabilisatieprofiel alleen binnen bereik is als de klimaatgevoeligheid aan de lage kant zit van die onzekerheidsband. Om het temperatuurdoel van de 2°C met grotere waarschijnlijkheid te kunnen halen, zou stabilisatie dus gericht moeten worden op 550 ppmv CO_2-equivalenten. Zonder het toestaan van een overshoot betekent dit stringente restricties voor de mondiale emissies, die niet later mogen pieken dan 2015 – 2020. Deze conclusies zijn ook afhankelijk van de aannames in de zwavelemissies, die niet worden meegenomen in het GWP-concept. In deze studie blijkt de onzekerheid door zwavelemissies niet groter dan 0.3°C te zijn, wat verwaarloosbaar is ten opzichte van de onzekerheid in de klimaatgevoeligheid. Voor onze conclusies hebben we aangenomen dat de niet-CO_2 broeikasgassen 100 ppmv CO_2-equivalenten bijdragen aan de stabilisatieniveaus. Uit een gevoeligheidsanalyse blijkt dat variatie in de bijdrage van niet-CO_2 broeikasgassen resulteert in een ander stabilisatieniveau (± 50 ppmv) en ook een andere temperatuurtoename (± 0.2°C) in de komende 100 jaar. Dit wordt verklaard door het feit dat het gebruik van GWP's, met een 100-jarig tijdshorizon, ervoor zorgt dat de bijdrage van kortlevende gassen zoals methaan wordt onderschat. Dit effect is minder zichtbaar op de langere termijn (meer dan 100 jaar), maar zorgt ervoor dat het GWP-concept minder goed bruikbaar is om temperatuurdoelen te vertalen naar equivalente broeikasgas emissiedoelen.

1. Introduction

1.1 Need for multi-gas stabilisation scenarios

Article 2 of the United Nations Framework Convention on Climate Change (UNFCCC) states that the ultimate objective of the Convention is '*to achieve stabilisation of greenhouse gas concentrations in the atmosphere at a level that would prevent dangerous anthropogenic interference with the climate system.*' There is much debate on the question of which concentrations of greenhouse gases can be regarded as safe and the conditions required for achieving these. Much of this debate has been covered in the Third Assessment Report (TAR) of the Intergovernmental Panel on Climate Change (IPCC, 2001c) by assessing scientific literature that researched the impacts of climate change. In fact, determining 'safe' levels is not only a scientific question but is also related to perceptions, values and political negotiations (Rayner and Malone, 1998). Most studies seem to agree that baseline emissions, without climate policy, will result in climate change and associated adverse impacts. Consequently, mitigation scenarios need to be developed to explore the required 'safe' level for stabilising greenhouse gas concentrations (Van Vuuren and De Vries, 2001).

Many previous studies into the 'safe emission' levels required to remain within a certain temperature change have only looked at CO_2 profiles (Enting et al., 1994; Wigley et al., 1996; Morita et al., 2000). However, we know that to study temperature increase we need to look at other greenhouse gases and radiative active gases (such as sulphur aerosols) as well. The IPCC has paid some attention to this issue in its TAR, but could only combine existing CO_2 profiles with baseline assumptions for non-CO_2 greenhouse gases (IPCC, 2001d). In view of the recent interest in non-CO_2 greenhouse gases (Hansen et al., 2000; Reilly et al., 1999) profiles need to be formulated not only for CO_2 but also for total greenhouse gases. Such profiles may serve a similar role in mitigation studies as CO_2 curves have in earlier studies. Some studies into constructing multi-gas emission profiles are now under way. As far as we know, Sygna et al. (2002) were the first to investigate how to link multi-gas profiles to long-term temperature targets. In this study we explore multi-gas profiles in a more systematic way than has been done so far.

1.2 Purpose of this study

In this study we present CO_2-equivalent emission profiles, calculated using Global Warming Potentials (GWP) on a time horizon of 100 years, that lead to CO_2-equivalent concentrations calculated using the radiative forcing for the Kyoto gases (CO_2, CH_4, N_2O, HFCs, PFCs and SF_6). The GWP concept was introduced to the scientific community in the first IPCC Assessment Report (IPCC, 1990) and was implemented in the Kyoto Protocol by the UNFCCC in 1997. The GWP is described as the comparison of the integrated radiative forcing of a pulse emission of a radiatively active species for a specific time horizon with the integrated radiative forcing of a CO_2 pulse emission. Although there is much debate on the concept of the GWP (Smith and Wigley, 2000a, Smith and Wigley, 2000b; Manne and Richels, 2001; Fuglestvedt et al., 2003), we used GWPs to calculate CO_2-equivalent emission profiles because simple economic models need this kind of information. Ideally, the share of CO_2 and non-CO_2 gases in CO_2-equivalent emission profiles does not matter. In this study we assess whether the use of CO_2-equivalent emission profiles leads to substantial differences in the global mean surface temperature increase in 2100, and whether this problem also occurs when CO_2-equivalent concentrations based on radiative forcing are used.

Box 1.1: Emission profiles versus stabilisation scenarios

In this report we describe the construction of emission profiles that are in line with the temperature target of 2 degrees Celsius. To construct these emission profiles we use a methodology that is mainly based on inverse calculations of the CO_2 emissions, as described in Enting et al. (1994). Since we focus on multi-gas emission profiles, we also determined the non-CO_2 greenhouse gas emissions. For this study we have made arbitrary assumptions to be able to compare our constructed multi-gas emission profiles with other CO_2-only emission profiles. Consequently, we assumed that non-CO_2 greenhouse gases will contribute 100 ppmv CO_2-equivalents (based on the sum of their radiative forcing effect). The resulting CO_2-equivalent emission profiles (based on the GWP concept) are evaluated in this study and are presented as multi-gas emission profiles that can serve as a basis for stabilisation studies, where the contribution of non-CO_2 greenhouse gases will be determined by cost optimisation calculations. An example of such a study is performed and described in Van Vuuren et al. (2003). This report forms the basis of that study.

Within the scope of this study we have only developed greenhouse gas emission profiles that stay within a 'safe' temperature range. Several studies have tried to help in determining the temperature increase corresponding to a level that would prevent dangerous anthropogenic interference with the climate system (IPCC, 2001b; Berk et al. 2001; O'Neill and Oppenheimer, 2002). This involves a considerable level of uncertainty. In addition, whether this level is regarded as 'safe' also involves political decisions. In this study we avoid this problem by evaluating the greenhouse gas stabilisation profiles that remain within a limit for the global mean surface temperature increase set at 2°C above the pre-industrial level. This level is in line with the goals of the climate policies of the European Commission (EC, 1996) and the Dutch government.

Which CO_2-equivalent concentration level leads to a rise in temperature of no more than 2°C above the pre-industrial level? To answer this we need to know the climate sensitivity that gives the equilibrium global mean surface temperature increase resulting from a doubling of CO_2-equivalent concentrations. Given the many uncertainties surrounding climate sensitivity, the IPCC has defined a range from 1.5°C to 4.5°C with 2.5°C as the medium value (IPCC, 2001a). Assuming a medium climate sensitivity, stabilisation of the CO_2-equivalent concentration level at around 560 ppmv leads to a temperature increase of 2.5°C (the pre-industrial CO_2-equivalent concentration is taken to be 280 ppmv). Based on this rough estimate, we decided to take the CO_2-equivalent concentration of 550 ppmv as our central case. Although stabilisation at 450 ppmv CO_2-equivalent may also lead to a 2°C increase we did not construct this emission profile because the current (2000) CO_2-equivalent concentration level is about 420 ppmv. Given the current annual increase in concentrations this means that stabilisation at 450 ppmv is only possible in profiles that first exceed this concentration level and later decline to 450 ppmv. As we have excluded 'overshoot' profiles from our analysis, we considered the 450 ppmv CO_2-equivalents out of range. We decided to analyse two stabilisation levels: 550 ppmv and 650 ppmv CO_2-equivalents. To compare our results with other emission profiles we broke down our 550/650 ppmv CO_2-equivalent profiles into 450/550 ppmv CO_2 and 100 ppmv non-CO_2 profiles. The calculated CO_2 emission profiles (leading to 450 and 550 ppmv CO_2) described in this report are compared with emission profiles determined using the Wigley, Richels & Edmonds profiles (WRE profiles) (Wigley et al., 1996).

We used the IMAGE 2.2 model (Alcamo et al., 1998; IMAGE team, 2001) to construct the emission profiles from pre-defined CO_2-equivalent concentration profiles. The IMAGE model (Integrated Model to Assess the Global Environment) is a system-dynamics oriented

integrated assessment model. It provides a reasonably elaborate description of the sources of greenhouse gas emissions, greenhouse gas concentrations, changes in radiative forcing and the resulting temperatures. The climate model is based on the MAGICC model (Hulme et al., 2000), which allows the climate sensitivity to be adjusted to investigate the consequences of uncertainties in the climate system.

1.3 Outline of the report

In Section 2 we review the theoretical background on CO_2-equivalent emissions and concentrations and briefly describe the IMAGE model. In Section 3 we describe how we constructed the emission profiles from pre-described concentration stabilisation levels and analysed the baseline used for the period from 2000 and 2100. Section 4 contains an analysis of the CO_2-equivalent emission profiles and their influence on the temperature increase. Section 5 explores the consequences of the range in climate sensitivities, different sulphur emission profiles and differences in the breakdown rates of CO_2 and non-CO_2 in the CO_2-equivalent emission profiles. In Section 5 we present our conclusions.

2. Theoretical background

2.1 CO$_2$ emission profiles
In 1994, Enting, Wigley and Heimann published the first coordinated attempt to determine
CO$_2$ emission profiles that lead to several CO$_2$ stabilisation levels (Enting et al., 1994). The
CO$_2$ concentration profiles, published in IPCC (1994), were called S350–S750 (which refers
to the CO$_2$ stabilisation levels) and had smooth transitions from the 1990 level (± 355 ppmv)
to the stabilisation level. In the second half of the 1990s discussions focused mostly on
whether early action was more effective than delayed response. Wigley et al. (1996; WRE
profiles) argued that postponing abatement action is always a more cost-effective strategy,
mainly because reduction options will become cheaper in the future. On the other hand,
others (e.g. Azar, 1998; Van Vuuren and De Vries, 2001) argued that early abatement can
significantly accelerate technology development.

Discussion of mitigation actions has focused on CO$_2$ – the most important greenhouse gas
(GHG) – until the late 1990s, when scientists claimed that mitigation analyses should include
full consideration of all major greenhouse gases (CH$_4$, N$_2$O, HFCs, PFCs and SF$_6$) as stated
in the Kyoto Protocol (Reilly et al., 1999). A full 'multi-gas' analysis was found to result in
significant cost reductions. In addition, Hansen et al. (2000) argued that a multi-gas analysis
may open up opportunities to have less global warming in the shorter term than analyses on
CO$_2$ alone because some gases have shorter atmospheric lifetimes. Despite these claims the
IPCC, in its TAR in 2001, used CO$_2$ stabilisation profiles from IPCC (1994) and Wigley et al.
(1996). To be able to calculate climate impacts, crude assumptions were made for the non-
CO$_2$ greenhouse gases: they follow the A1b path until 2100 and thereafter remain constant
(IPCC, 2001c). Morita et al. (2002) studied different post-SRES mitigation scenarios, but
only with policies for reducing CO$_2$ emissions. In all these studies the Kyoto Protocol
reductions were not included either.

Given this history, there is a need to update the emission profiles. Most importantly, we need
emission profiles resulting in a stabilisation of the radiative forcing while taking into account
all the Kyoto gases. Moreover, besides an updated base year (from 1990 to 2000), GHG
profiles may need to take the Kyoto Protocol into account (i.e. a reduction for some countries,
baseline for others).

2.2 CO$_2$-equivalent emission profiles
To compile stabilisation profiles that take all the Kyoto gases into account we need to resolve
how to add up the emissions from different gases. In this report we use two terms: CO$_2$-
equivalent emissions and CO$_2$-equivalent concentrations. For CO$_2$-equivalent emissions we
make use of the Global Warming Potential (GWP) of each Kyoto gas. GWP is defined as the
integrated radiative forcing of a pulse emission of a radiatively active species for a specific
time horizon compared with the integrated radiative forcing of a CO$_2$ pulse emission (i.e. the
GWP of CO$_2$ is by definition 1.0). We used the GWPs with a time horizon of 100 years given
in the TAR (IPCC, 2001a). Appendix A contains more details on the mathematics.

The introduction of the GWPs prompted a scientific debate on whether they are a good
measure for combining the various effects of different greenhouse gases on the climate
system. Smith and Wigley (2000a) provide a good review of the scientific problems of
GWPs. They argue that the limitations of GWPs can be divided into definitional problems,
quantification uncertainties and mathematical problems. Definitional problems arise from the

fact that the use of global GWPs ignores explicit geographical differences in the impacts of, for example, SO_2 emissions. Smith and Wigley also argue that the derivation of GWP involves many quantitative uncertainties, mainly in the gas-cycle modelling (e.g. lifetime uncertainties). Finally, they argue that the use of GWPs leads to substantial errors in the longer term (especially for short-lived gases such as CH_4). The main reason is that the GWPs account for the cumulative effect of greenhouse gases on the radiative forcing. This cumulative effect can never decrease over an infinite time horizon (it will reach a constant value); once it is emitted, the contribution of a GHG is fully accounted for and no further decrease can occur. This is not the case in the atmosphere: on an infinite time scale, every emission pulse will be removed from the atmosphere and, after reaching an equilibrium state again, the influence of the greenhouse gas pulse on the global mean temperature change will be zero. The discussion on the use of GWPs is still very lively, as shown by Fuglestvedt et al. (2003), Smith (2003)and O'Neill (2003), who give a good overview of the different problems arising from the use of GWPs.

Despite these difficulties, the use of GWPs has some important advantages, the main one being the easy method for calculating and interpreting CO_2-equivalent emissions. Most studies that have assessed possible alternatives conclude that at the moment no good alternatives exist that take the different effects of GHGs on the climate system into account and are as easy for modellers and policy makers as using GWPs.

In this report we also use CO_2-equivalent concentrations, which express the radiative forcing of all greenhouse gases as an equivalent CO_2 concentration that would result in a similar forcing (see Appendix A for the equations). This approach allows us to include all compounds influencing the radiative forcing (i.e. aerosols and ozone precursors), but we do not consider the consequences of this possibility in this study. After emitting the Kyoto gases, the concentration and the radiative forcing of each Kyoto gas are calculated. Because of different rates of removal from the atmosphere of each greenhouse gas the CO_2-equivalent concentration can decrease whereas CO_2-equivalent emissions can never decrease (see above). Therefore, the effect of different contributions of Kyoto gases (with an equal total amount of CO_2-equivalent emissions) can lead to different levels of CO_2-equivalent concentrations. In this study this effect is assessed in Chapter 5 by using the more complex IMAGE model (see Box 2.1), which also models atmospheric gas-cycles (see Eickhout et al., 2003).

Box 2.1: The IMAGE 2.2 model

The purpose of the IMAGE 2.2 model (Integrated Model to Assess the Global Environment, IMAGE team, 2001) is to explore the long-term dynamics of global environmental change. The model contains several disciplinary models (Figure 2.1) and delivers results for 17 socio-economic regions (plus Antarctica and Greenland). The IMAGE model consists of four main components:

- The Energy-Industry models calculate regional energy consumption, energy efficiency improvements, fuel substitution, and the supply of and trade in fossil fuels and renewable energy technologies. Data on energy use and industrial production are used to calculate emissions of GHGs, ozone precursors and sulphur (De Vries et al., 2001).
- The ecosystem, crop and land use models dynamically compute land use from data on regional consumption, production and trade of food, animal feed, fodder, grass and timber, and local climatic and terrain properties. Emissions from land use change, natural ecosystems and agricultural production systems, and the exchange of CO_2 between terrestrial ecosystems and the atmosphere are computed (Alcamo et al., 1998).
- The atmospheric and ocean models calculate changes in atmospheric composition using emissions data and take oceanic CO_2 uptake and atmospheric chemistry into consideration. Changes in climatic properties are then computed by resolving the changes in radiative forcing caused by GHGs, aerosols and oceanic heat transport. The climate model implemented in IMAGE 2.2 is based on the MAGICC model (Hulme et al., 2000). For further details on the implementation in IMAGE see Eickhout et al. (2003).
- The impact models involve specific models for sea level rise and land degradation and make use of specific features of the ecosystem and crop models to depict impacts on vegetation. The ecosystem models include an algorithm that estimates the carbon cycle consequences of different assumptions on the speed of climate change induced vegetation migration (Van Minnen et al., 2000).
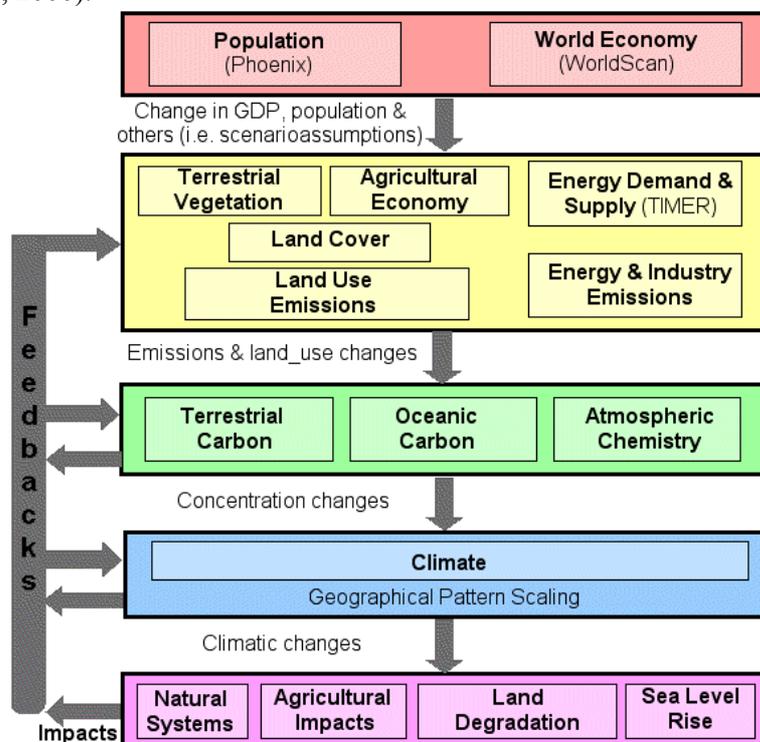

Figure 2.1: The structure of the IMAGE 2.2 framework (IMAGE team, 2001).

3. Methodology: Constructing the emission profiles

Emission profiles for two concentration levels (550 ppmv and 650 ppmv CO_2-equivalents) have been developed using the IMAGE 2.2 model. The basis of our calculations is the Common POLES-IMAGE (CPI) baseline (without climate policies; see Section 3.1). In Sections 3.2, 3.3 and 3.4 we describe how we constructed the CO_2-equivalent emission profiles that lead to stabilisation of CO_2-equivalent concentrations.

3.1 General methodology

For several reasons we need to specify the baseline from which the stabilisation regimes have been derived. First, baseline assumptions on population growth and technology changes determine future land use through agricultural activities. Land use is important since it affects the carbon cycle, notably the uptake of carbon from the atmosphere by the biosphere (terrestrial carbon uptake), and it affects non-CO_2 GHG emissions (e.g. methane from animals and rice paddies and N_2O from agricultural fertilisers). Second, the baseline influences the emissions of non-participating countries during the Kyoto period (i.e. the non-Annex I countries and the US between 2000 and 2010)

For this study we used the CPI baseline (Van Vuuren et al., 2003) developed by RIVM and the French Institute de l'Economie et de Politique de l'Energie (IEPE). This baseline describes trends in the main driving forces (population and economic growth), environmental pressures (energy, industrial and land use emissions) and their resulting effects, such as temperature increase, for the 1995–2100 period. It is derived from the existing POLES reference scenario to 2030 (see Criqui and Kouvaritakis, 2000) and the IMAGE B2 scenario from 2000 to 2100 (IMAGE team, 2001; Nakicenovic et al., 2000). This baseline does not include any climate policies and runs from 1970 to 2100, with calibration to data from 1970 to 2000. Table 3.1 summarises the main characteristics of the CPI baseline. The population scenario assumes that the global population stabilises at a level of 9.5 billion by 2100. On the economic side, the CPI baseline scenario describes a world in which globalisation and technological development continue to be important factors underlying economic growth, although not as strong as assumed in the IPCC A1b scenario (IMAGE-team, 2001; Nakicenovic et al., 2000). As a consequence, the economic growth rate in the Annex I regions varies between 1.5 and 2.0% in the 1995–2025 period and slows down somewhat after 2025 to around 1.0 to 1.2%. Growth rates for Asia, South America and North Africa and the Middle East are significantly higher and vary between 2.0 and 4.0% (see Table 3.1).

Table 3.1: Main driving forces by CPI baseline region.

	Population (x 10^6)			Per Capita Income (in PPP 1995 $/year)			Per Capita Income (growth rates annually)	
	1995	2025	2050	1995	2025	2050	1995-2025	2025-2050
Canada	29	37	41	19047	30971	39023	1.6%	0.9%
USA	267	325	350	26316	43835	57717	1.7%	1.1%
Central America	159	235	273	2550	5556	10199	2.6%	2.5%
South America	317	455	527	4113	7411	13152	2.0%	2.3%
North Africa	131	205	251	1203	2461	4974	2.4%	2.9%
Western Africa	282	547	757	306	371	852	0.6%	3.4%
Eastern Africa	172	333	462	221	272	657	0.7%	3.6%
Southern Africa	134	261	361	1186	1443	2844	0.7%	2.8%
Western Europe	384	382	346	21636	42224	58364	2.3%	1.3%
Central Europe	121	117	104	2822	9426	22638	4.1%	3.6%
Former SU	293	298	273	1747	5323	14750	3.8%	4.2%
Middle East	219	378	483	3282	6371	12577	2.2%	2.8%
South Asia	1245	1865	2160	356	1560	4060	5.0%	3.9%
East Asia	1316	1616	1638	1360	8434	19145	6.3%	3.3%
South-East Asia	482	677	801	1478	4944	12401	4.1%	3.7%
Oceania	28	40	46	15469	30054	43397	2.2%	1.5%
Japan	125	121	111	41052	65270	90424	1.6%	1.3%
World	5706	7891	8984	4931	9052	14413	2.0%	1.9%

The following sections describe the methodology for constructing emission profiles. Figure 3.1 shows the four phases identified in the methodology. In phase I (from 1970 to 2000) historical emissions data are used to set the scene. These emissions include the recent slowdown in GHG emission growth towards the end of the last century, in particular resulting from the strong reductions in emissions in the Former Soviet Union (FSU) and Eastern Europe following their economic decline and the reductions in CO_2 emissions in China during the second half of the 1990s. Given the projected increase in population and income, this decrease in emissions is considered to be a temporary phenomenon, with future emission projected to increase substantially again.

In phase II, from 2000 to 2010, climate policies are implemented for those countries that have agreed to them. The countries that do not implement any climate policy follow the CPI baseline. Table 3.2 contains a summary of the CPI baseline emissions. More details on the period from 2000 to 2010 are given in section 3.2.

I : Historical emissions

II : CPI baseline and Kyoto implementation

III : From annual increase to annual decrease
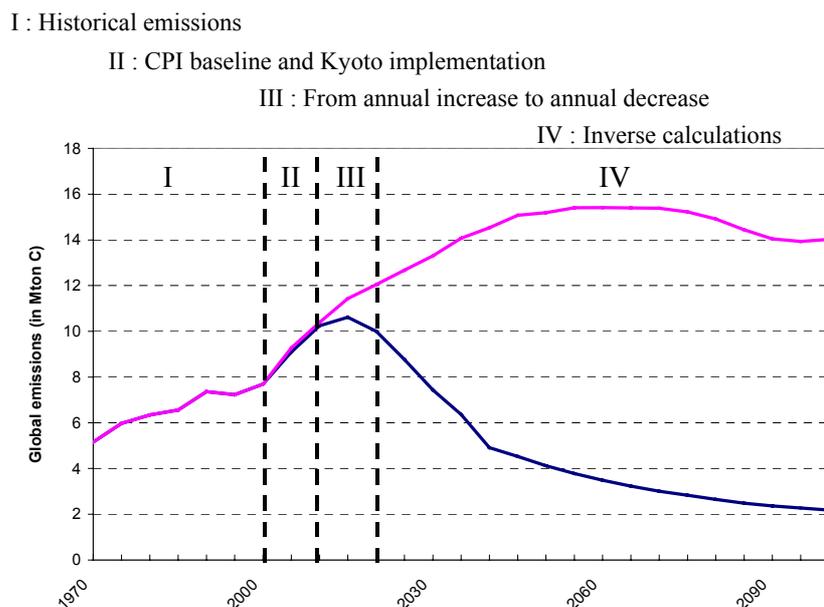
IV : Inverse calculations

Figure 3.1: Schematic sketch of the general methodology used for the construction of the emission profiles, distinguishing four different phases from 1970 to 2100.

In phase III it is assumed that post-Kyoto policies bring about more ambitious emission reductions. These reductions are achieved by assuming a shift from an annual emission increase to a certain annual emission decrease. The year in which emissions peak and the size of the annual emission decrease depend on the stabilisation level (see Section 3.3). Finally, in phase IV, global emissions are calculated by using inverse calculations of the IMAGE model. A pre-defined concentration path (with a certain stabilisation level) forms the basis for calculating back the global emissions (see Section 3.4).

Table 3.2: Main model results by CPI baseline region.

	CO_2 emissions (in $GtCO_2$/year)			GHG emissions (in $GtCO_2$-eq/year) *		
	1995	2025	2050	1995	2025	2050
Canada	0.48	0.62	0.70	0.73	0.77	0.55
USA	5.39	7.19	7.52	7.04	8.43	7.88
Central America	0.40	0.95	1.61	1.10	1.43	2.09
South America	0.70	1.76	3.30	2.35	3.23	4.29
North Africa	0.26	0.62	1.03	0.40	0.92	1.32
Western Africa	0.11	0.51	0.95	0.81	3.74	5.54
Eastern Africa	0.04	0.15	0.48	0.40	1.32	1.06
Southern Africa	0.33	0.95	1.91	0.73	2.31	2.97
Western Europe	3.34	3.92	4.07	4.33	4.51	4.47
Central Europe	0.77	0.92	1.03	1.03	1.14	0.95
Former SU	2.24	3.15	3.52	3.41	3.92	3.48
Middle East	0.99	2.68	4.14	1.39	3.67	5.72
South Asia	0.92	3.67	7.26	2.38	5.90	9.61
East Asia	3.56	8.62	11.15	6.12	11.62	13.02
South-East Asia	0.62	1.91	4.07	1.47	4.40	6.12
Oceania	0.33	0.51	0.62	0.48	0.66	0.66
Japan	1.14	1.36	1.32	1.36	1.58	1.50
World	21.56	39.53	54.74	35.97	60.87	74.10

*: The GHGs included here are the 6 Kyoto gases: CO_2, CH_4 $_2O$, SF6, PFCs; HFCs. However, the F-gases are excluded from the regional figures because only global estimates are made. This means that the regional subtotals do not add up to the world total.

Until 2100 the CO_2 land use emissions follow the CPI baseline. Therefore, the assumptions relating to land use determine the amount of carbon that is emitted and sequestered during the 21st century. In general, population growth and a shift towards more luxurious diets increases the area of agricultural land needed during the first half of century, despite improvements in agricultural production. Later, further productivity gains result in a more excess agricultural land than can be converted into forest, particularly in high-income regions. As a result, CO_2 emissions from land use increase slightly between 1995 and 2040, but decrease thereafter. The CPI baseline emissions are depicted in Figure 3.2.
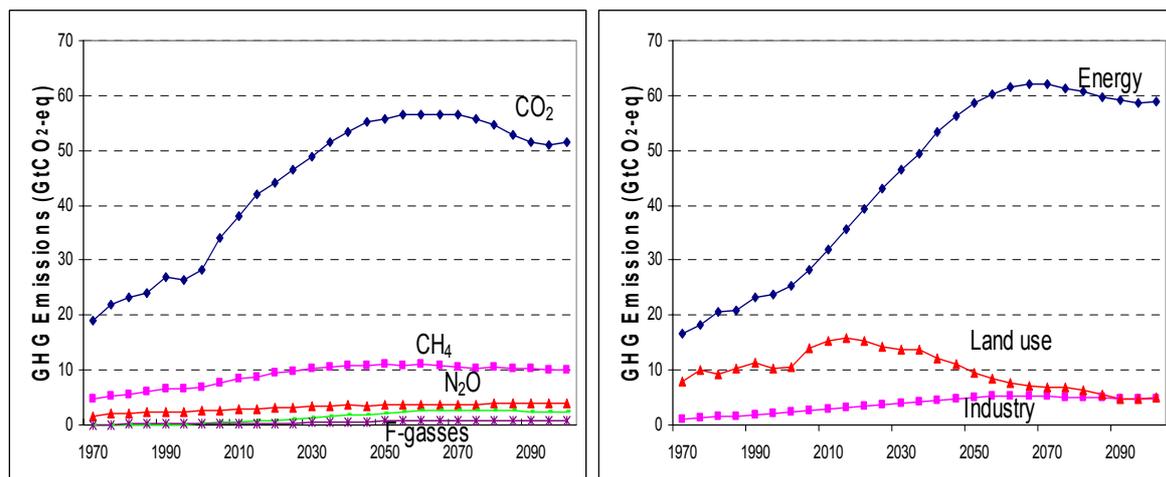

Figure 3.2: Greenhouse gas emission in carbon-equivalents by gas (left) and by sector (right).

3.2 Implementation of current climate policies until 2010

In contrast to the baseline, for the stabilisation profiles we assumed that recent climate policies – the Kyoto Protocol and the Bush Climate Initiative – will be fully implemented from 2000 to 2010: all Annex I countries except the US meet their Kyoto targets and the United States reduces 'greenhouse gas intensity' by 18% in the 10-year period. For the exact implications of the Kyoto Protocol we used the quantified emission limitations or reductions as a percentage of the base year or 1990 emissions. This takes into account the corrections that follow from specific articles of the Kyoto Protocol on country-specific base years other than 1990 and the sink credits under the Marrakesh Accords (Den Elzen and De Moor, 2002). The Kyoto Protocol allows countries to bank 'hot air'.[1] In our analysis we assumed that Eastern Europe and the FSU will bank hot air optimally to maximise revenues (exercise market power by limiting the supply of hot air and so raise the prices of emission permits), leading to 80% banking of hot air. Using the results of the FAIR model (Den Elzen and Lucas, 2003) we determined the new emission reduction goals for Eastern Europe and the Former Soviet Union. In Table 3.3 the emission reduction targets are compared with the 1990 emission levels of the Annex I countries. It is assumed that these new emission reduction goals are met in 2010 (the middle of the first Commitment Period).

---

[1] Because of the economic downturn in the early 1990s, the Annex I countries of the former Soviet Union (FSU), that is Russia, Ukraine, Latvia, Lithuania and Estonia, are emitting substantially less CO_2 and their emissions in 2010 are expected to be well below their Kyoto targets. Although this is sometimes referred to as surplus allowances, the term 'hot air' is mostly commonly used.

Table 3.3: Emission reduction targets compared with 1990 levels for the Annex I countries, taking into account the US withdrawal (see Den Elzen and De Moor, 2002)

Annex I Region	Original Kyoto target	Targets compared to 1990 with optimal hot air banking
Canada	-6.0%	-6.0%
OECD'90 Europe	-7.8%	-7.5%
Eastern Europe	-7.1%	banking
Former Soviet Union	-0.2%	banking
Oceania	+6.8%	+22.1%
Japan	-6.0%	-4.9%

It is assumed that Eastern Europe and the FSU only bank fossil CO_2 emissions and so emissions from CH_4 and N_2O follow the baseline as described in Section 3.1. Furthermore, it is assumed that all other Annex I countries meet their targets for fossil CO_2, anthropogenic CH_4 and anthropogenic N_2O separately. Given this assumption, all Annex I countries mentioned in Table 3.3 (except for Eastern Europe and FSU) will have to take action to reach their targets for fossil CO_2 emissions. For CH_4 and N_2O this is not always the case, since some of the industrial and/or land use emissions for these gases are below the targets for the baseline. Please note that no emission reductions in HFCs, PFCs and SF_6 are assumed because IMAGE 2.2 only uses global emissions data for these gases.

3.3 CO_2 emissions after 2010: when will they peak?
After 2010 we assume emission reductions are introduced to reach the pre-defined concentration levels. The time taken for GHG concentrations to stabilise were adopted from IPCC for CO_2 to allow for comparison between the stabilisation profile for CO_2 only and for all GHGs. The 550 ppmv CO_2-equivalent concentration level (450 ppmv CO_2 and 100 ppmv CO_2-equivalents for CH_4, N_2O and F-gases) is reached in 2100 and the 650 ppmv CO_2-equivalent concentration level (550 ppmv CO_2 and 100 ppmv non-CO_2) is reached in 2150.[2]

After 2010 we distinguish two phases in the constructed emission profiles:
1) The growth of CO_2 emissions shifts from an annual increase in 2010 to a maximum annual decrease of 2% .
2) After this first phase, CO_2 emissions are derived using an inverse calculation by the IMAGE 2.2 model, determining the allowable emission levels resulting from a pre-described CO_2 concentration profile.

We assumed that an optimal reduction pathway over the century should not exceed an annual reduction in global emissions of 2% per year (at least not over longer time periods). The reason is that a faster reduction is difficult to achieve given the inertia in the energy system: electric power plants, for instance, have a technical lifetime of 30 years or more. Fast reduction rates would require early replacement of existing plants, which is expensive. In order to get an impression of the maximum reduction rates in long-term emission scenarios we plotted the annual emission reduction rates (30 year averages) for a set of 18 emissions reduction scenarios (Morita et al., 2000). These scenarios were constructed using a large number of different models and aim for stabilisation of the atmospheric CO_2 concentration at 450–750 ppmv CO_2. To remain consistent with the stabilisation levels chosen for in this

---

[2] Note that 650 ppmv stabilisation in 2150 leads to a much smoother profile than stabilisation in 2100. The latter would require relative high emissions during the initial decades (to reach a high enough concentration level) followed by steep emission reductions in the second half of the century to stabilise concentrations.

report, we only looked at the scenarios that aim for stabilisation at 450 ppmv and 550 ppmv CO_2 (13 scenarios; see Figure 3.3).
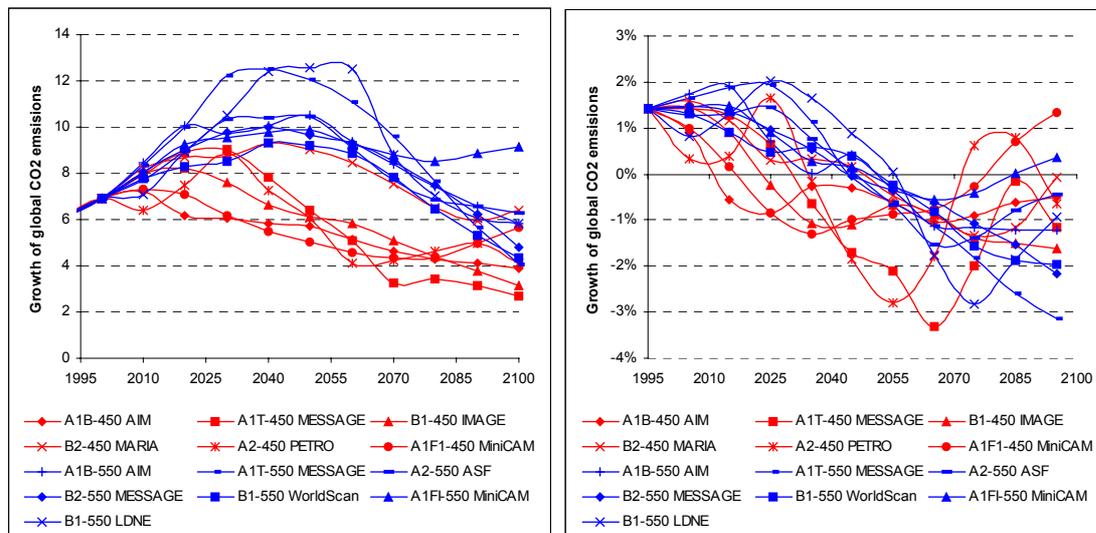

Figure 3.3: Global energy-related CO_2 emissions scenarios that aim to stabilise the greenhouse gas concentration at 450 ppmv and 550 ppmv CO_2, in terms of their emissions (left) and 20-year average annual reduction rates (right; Morita et al., 2000).

Figure 3.3 shows that the 2% rate of decrease is hardly exceeded across the total set. Some exceptions occur for 450 ppmv stabilisation scenarios that have a relatively fast reduction period around 2050 (the A1T-450 MESSAGE scenario and the A2-450 PETRO scenario) and one 550 ppmv stabilisation scenario that postpones mitigation action to the very last decades (A1T-550 MESSAGE). In all cases this rate is only kept for a limited period of time. This is illustrated by converting the data in Figure 3.3 into a histogram showing reduction rates (Figure 3.4; data from 2025 to 2100).
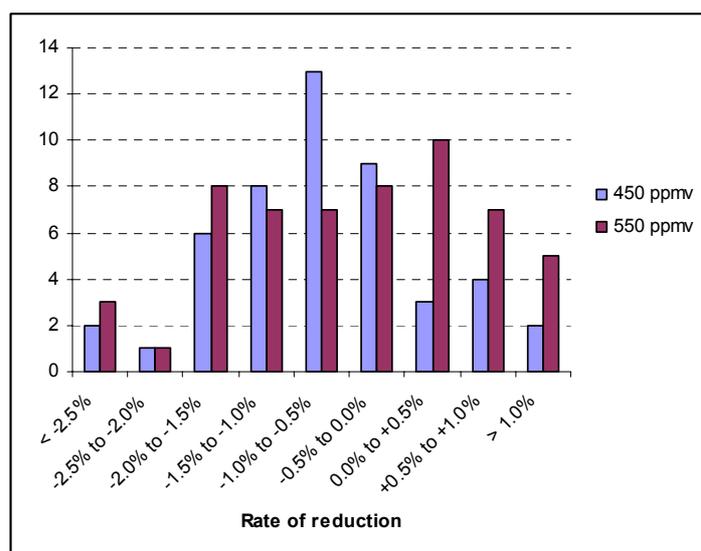

Figure 3.4: Histogram of the rate of reduction in the 2025-2100 period across the reduction scenarios of the post-SRES set leading to stabilising at 450 and 550 ppmv stabilisation of the CO_2 concentration (data from Figure 3.3).

Stabilising concentrations of CO_2-equivalents at 550 ppmv in 2100 requires steep reductions after implementation of the Kyoto Protocol and the Bush Climate Change Initiative. In 2010 the CO_2 concentration is already above 390 ppmv, which means fast emission reductions thereafter. For the 650 ppmv CO_2-equivalents level in 2150 we had more scope for adjustment. To prevent stringent emission reductions we assumed that the CO_2 emissions have to reach a 1.5% annual decrease in 2040. Consequently, the global emissions peak in different years: around 2015 in the case of 550 ppmv CO_2-equivalents and around 2025 in the case of 650 ppmv CO_2-equivalents.

3.4 Calculating CO_2 emissions from CO_2 concentration pathways

Phase IV of the emission profiles is determined using the method described by Enting et al. (1994). The CO_2 concentration profile is determined using a Padé approximant (Eq. 3.1).

$$[CO_2](t) = \frac{a + bx + cx^2}{1 + dx + ex^2} \qquad\qquad (3.1)$$

with:

$$x = \frac{t - t_0}{t_{stab} - t_0}$$

$[CO_2]$ = calculated CO_2 concentration (ppmv)
t = calculated year (yr)
t_0 = start year of stabilisation profile (yr)
t_{stab} = year of stabilisation (yr)

The values of a, b, c, d and e can be calculated because five points of the concentration profile are pre-described:

1. the CO_2 concentration in the starting year (2010; ppmv);
2. the gradient of the CO_2 concentration profile in the starting year (2010; ppmv per year);
3. the CO_2 concentration in the year of stabilisation (ppmv);
4. the gradient in the year of stabilisation (0.0 ppmv per year);
5. the CO_2 concentration in a year in between (ppmv).

The reader is referred to Appendix B for more details on the calculation of the values in Equation 3.1 using the 5 constraints. Table 3.4 summarises the assumptions we used to reach stabilisation levels in 2100 and 2150 for the 550 and 650 cases respectively. Using inverse calculations of the IMAGE 2.2 model we calculated the resulting fossil CO_2 emissions using the CO_2 concentration profile as input. The terrestrial and oceanic carbon cycle models (see Figure 2.1) of IMAGE 2.2 calculate the corresponding terrestrial and oceanic carbon fluxes.

Table3.4: *Defined values in Padé approximants to calculate CO_2 concentration stabilisation profiles, based on Enting et al. (1994).*

Parameter in Padé approximant	CO₂ 450 ppmv stabilisation profile	CO₂ 550 ppmv stabilisation profile
t_0	2025	2040
$[CO_2](t_0)$	427.0 ppmv	486.9 ppmv
$\Delta[CO_2](t_0)$	1.5 ppmv/yr	1.6 ppmv/yr
t_{stab}	2100	2150
$[CO_2](t_{stab})$	450.0 ppmv	550.0 ppmv
$\Delta[CO_2](t_{stab})$	0.0 ppmv/yr	0.0 ppmv/yr

3.5 Reductions in non-CO$_2$ greenhouse gases after 2010

We assumed that non-CO$_2$ greenhouse gases are responsible for a further 100 ppmv CO$_2$-equivalent in each stabilisation profile. As the lifetimes of the GHGs differ greatly the distribution among the gases is important for our final outcomes. As we did not apply a full costs optimisation over time, we assumed reduction rates based on expert judgement. Until 2010, the non-CO$_2$ greenhouse gases for the non-Annex-I countries are determined by the baseline (Section 3.1) and for the Annex-I countries by the implementation of the Kyoto Protocol (Section 3.2).[3]

After 2010 mitigation options are applied to non-CO$_2$ emission categories that are assumed to be easy to reduce. These emission reductions are applied to get to a contribution of 100 ppmv CO$_2$-equivalent concentration by the non-CO$_2$ greenhouse gas emissions. For methane these are all emissions from energy and industry and emissions from landfills and sewage. For nitrous oxide these are all emissions from energy and industry, emissions from sewage and emissions from fertiliser use. It is assumed that emission reductions in the developing countries will be slower than in the developed countries. Table 3.5 compares the assumed emission reductions for CH$_4$ and N$_2$O with the baseline.

Table 3.5: Assumed emission reductions compared with the CH$_4$ and N$_2$O baseline profile. The reduction percentage remains constant after the target years.

Emission category	Annex-I	Non-Annex-I
CH$_4$ energy and industry	-50% in 2025	-50% in 2040
CH$_4$ landfills	-100% in 2025	-100% in 2040
CH$_4$ sewage	-50% in 2025	-50% in 2040
N$_2$O energy and industry	-50% in 2025	-50% in 2040
N$_2$O sewage	-100% in 2025	-100% in 2040
N$_2$O fertiliser use	-20% in 2025	-20% in 2040

Emission reductions in HFCs, PFCs and SF$_6$ are determined in a similar way to the emission reductions for methane and nitrous oxide. However, in these emission profiles of the F-gases a distinction has been made between the two stabilisation profiles. This distinction is needed because the natural N$_2$O emissions in the highest profile are higher than in the 550 CO$_2$-equivalent profile as a result of the higher temperature in the 650 CO$_2$-equivalent profile. The higher temperature in this profile causes more soil respiration of N$_2$O. To compensate for these higher N$_2$O emissions, it is assumed that the reductions in HFC and PFC emissions reach a level of 100% in 2100. In the lower profile of 550 CO$_2$-equivalents only a 50% reduction is reached in 2100.

3.6 Summary of the emission profiles

Table 3.6 summarises the main characteristics of the constructed GHG stabilisation profiles. In Figures 3.5 and 3.6 the resulting CO$_2$-equivalent concentration levels and the coinciding CO$_2$-equivalent emissions are plotted alongside the results for the CPI baseline for comparison. The consequences for the global-mean temperature change are discussed in Chapter 4. For this analysis we also have to look at the sulphur emissions because SO$_2$ aerosols have a negative impact on radiative forcing. The negative health effects and environmental impacts of SO$_2$ emissions make it hard to believe that no SO$_2$ emission reductions will take place in the coming 100 years. When carbon intensive energy sources like coal are phased out to achieve CO$_2$ emission reductions in the stabilisation profiles, SO$_2$

---

[3] Since only global estimates are available for the HFCs, PFCs and SF$_6$ in the baseline, these gases follow the baseline completely until 2010.

emissions will also be reduced. In the stabilisation profiles we assumed the ratio between energy and industry related SO_2 reductions will be the same as for energy and industry related CO_2 reductions, compared with the baseline. The assumption of an equal $CO_2 : SO_2$ ratio in emission reductions by the energy and industry sectors was checked against other IMAGE mitigation scenarios defined by the IMAGE energy demand model TIMER (De Vries et al., 2001). In these scenarios the energy related SO_2 reductions were even slightly bigger than the energy CO_2 reductions. This supports the assumption that the same ratio for emission reductions from the energy and industry sectors is reasonable.

Table 3.6: Main characteristics of the two constructed emission profiles.

Characteristic	IMAGE S550e	IMAGE S650e
CO_2 emissions in 2010 (GtCO_2 per year)	37.58	37.58
Annual increase in 2010 (in %)	1.95	1.95
Target year of pre-described annual decrease CO_2	2020	2040
Level of annual CO_2 decrease in that target year (in %)	2.0	1.5
Year of stabilisation	2100	2150
Level of CO_2 concentration	450 ppmv	550 ppmv
Assumed levels of CH_4 reductions (compared to baseline)[1]	• Energy: 50% • Industry: 50% • Landfills: 100% • Sewage: 50%	• Energy: 50% • Industry: 50% • Landfills: 100% • Sewage: 50%
Assumed levels of N_2O reductions (compared to baseline)[1]	• Energy: 50% • Industry: 50% • Sewage: 100% • Fertiliser: 20%	• Energy: 50% • Industry: 50% • Sewage: 100% • Fertiliser: 20%
Level of reduction for HFCs and PFCs in 2100 (reduction percentage compared to baseline)	50%	100%[2]
Sulphur emission levels	Constant CO_2/SO_2 ratio	Constant CO_2/SO_2 ratio

[1] Reached in 2025 for Annex I and in 2040 for non-Annex I.
[2] Reductions in F-gases are higher in IMAGE S650e to compensate for higher natural N_2O emissions resulting from a larger temperature increase.
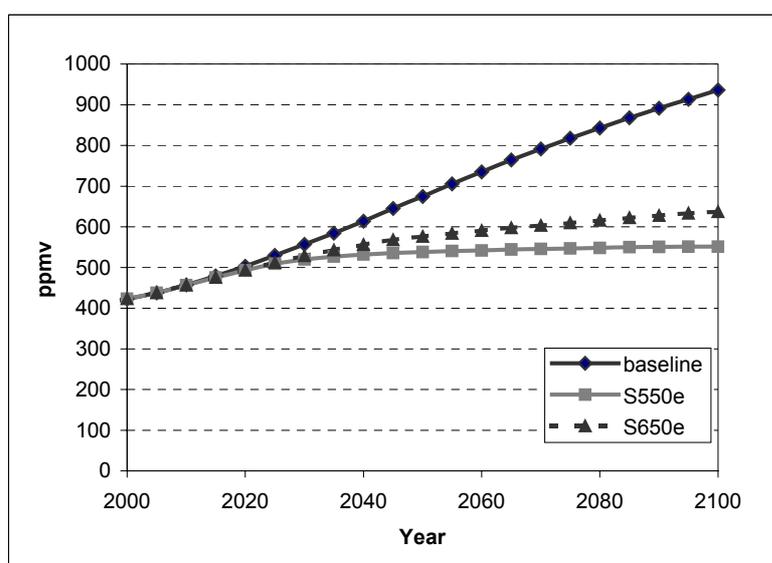

Figure 3.5: Global CO_2-equivalent concentration stabilisation profiles for S550e and S650e ppmv compared with the CPI baseline scenario.

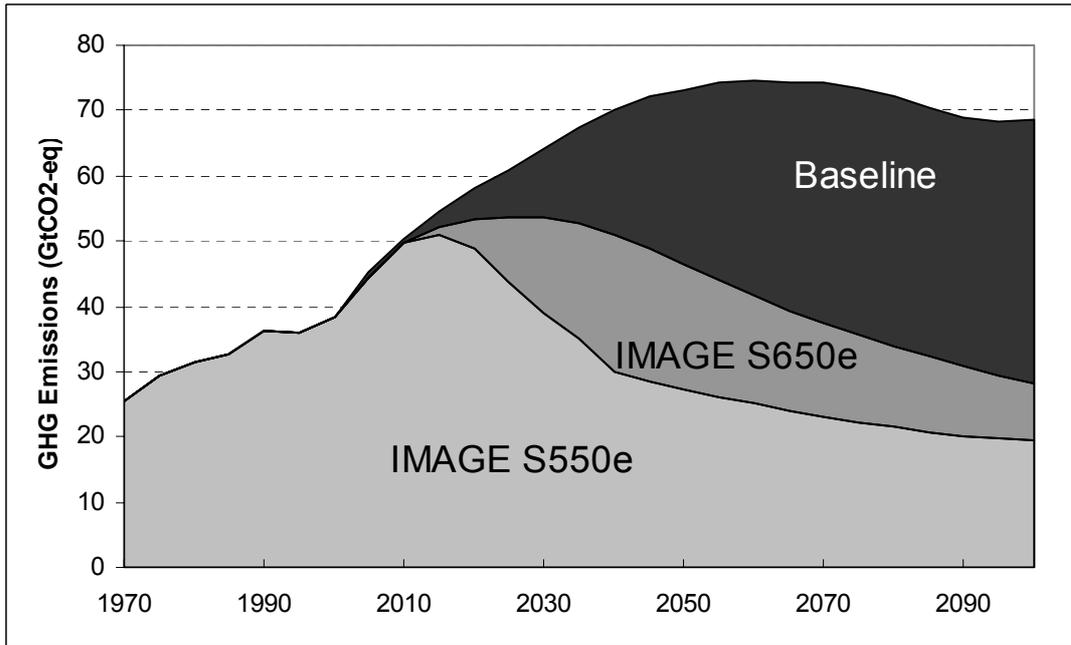*Figure 3.6: Global emission profiles for stabilising GHG concentrations at 550 ppmv (IMAGE S550e) and 650 ppmv (IMAGE S650e)compared with baseline emissions.*

4. Analysis of the greenhouse gas emission profiles

In this Chapter, we analyse the emission profiles reported in Chapter 3. We compare our results with the IPCC profiles (IPCC, 1994) and the WRE profiles (Wigley et al., 1996) in Section 4.1. This is followed by a discussion of the consequences for the increase in global mean temperature (Section 4.2) and the emission reduction burden (Section 4.3).

4.1 The CO_2-equivalent emission profiles

Figures 4.1 and 4.2 compare the two CO_2-only emission profiles with the corresponding 'early action' profile of the IPCC (1994) and the 'delayed response' profile of Wigley, Richels and Edmonds (WRE), of which the latter is commonly used in the IPCC-TAR. Interestingly, the CO_2 emissions in the IMAGE 450 ppmv profile peak somewhat later and at a higher level than in the WRE 'Delayed Response' profile, followed by steeper emissions reductions. The main reason for this is that in this analysis the developing countries follow their baseline until 2010. This implies that reductions are already somewhat delayed compared with the WRE 'Delayed Response' profile. Compared to the IPCC S450 profile the IMAGE profile can be really characterised as 'delayed response'.
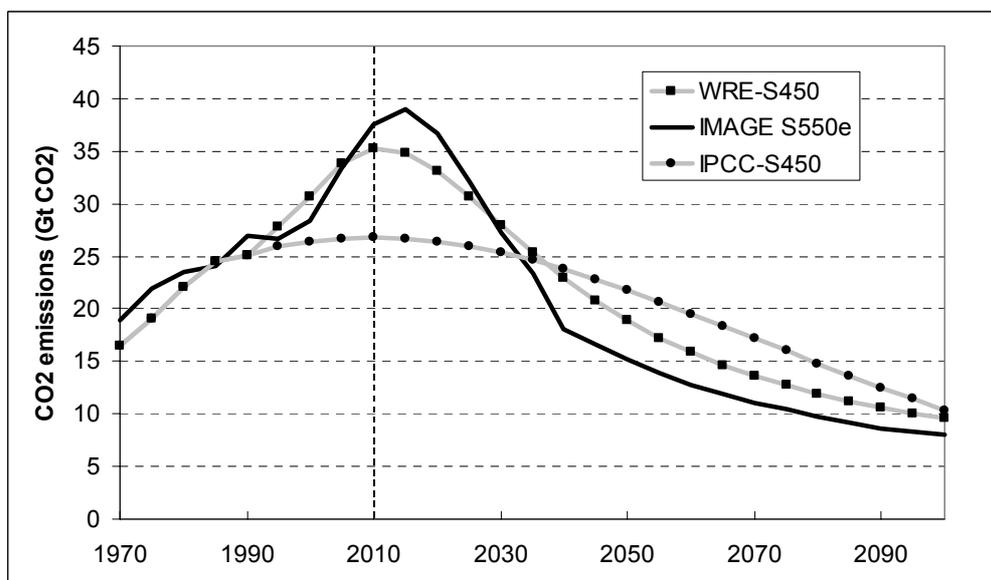

Figure 4.1: The comparison of the constructed IMAGE profile and the WRE Delayed Response emission profile, leading to 450 ppmv CO_2 in 2100.

The 550 ppmv CO_2 IMAGE profile (from the IMAGE S650e profile) is very similar to the 550 ppmv CO_2 WRE profile, this in contrast to the IPCC 550 ppmv CO_2 profile (Figure 4.2). In Table 4.1 the characteristics of the IMAGE profiles and the WRE profiles are compared using indicators mentioned in the IPCC Synthesis Report (IPCC, 2001d).

Table 4.1: Characteristics of the IMAGE 2.2 stabilisation profiles compared with the characteristics of the WRE profiles, as calculated by two IPCC models in the Synthesis Report (IPCC, 2001d)

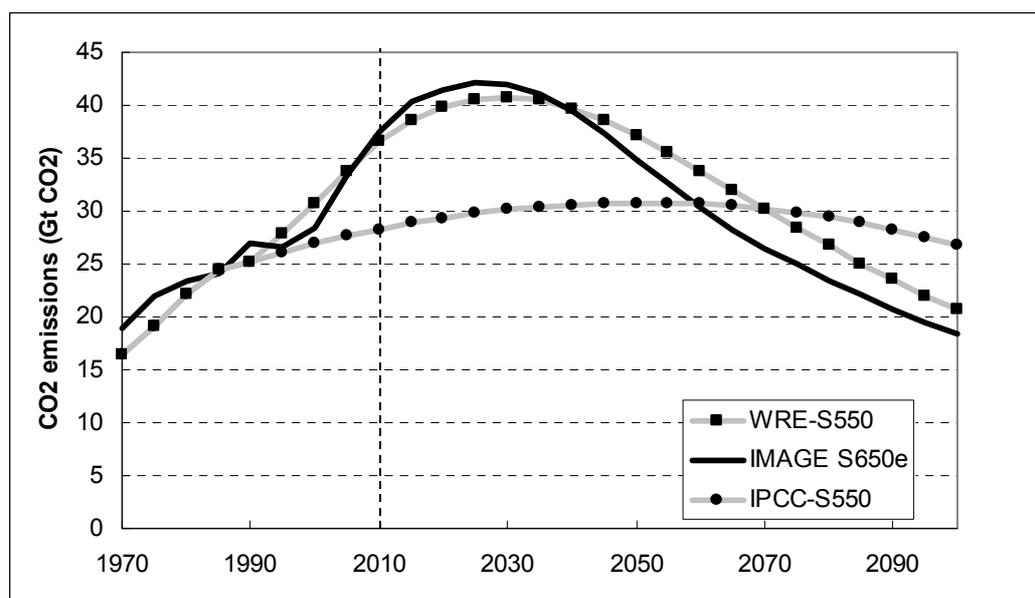| Stabilisation profile (in ppmv CO_2 equivalent)	CO_2 emissions (GtC/yr)		Accumulated CO_2 emissions (Gt C)	Year in which emissions	
	2050	2100	2001-2100	Peak	Fall below 1990 levels
550-IMAGE	4.1	2.2	530	≈2015	2030–2035
450-WRE	3.0–6.9	1.0–3.7	365–735	2005–2015	<2000–2045
650-IMAGE	9.3	5.2	870	≈2030	2070–2075
550-WRE	6.4–2.6	2.7–7.7	590–1135	2020–2030	2030–2100

Figure 4.2: Comparison of the constructed IMAGE emission profile and the WRE Delayed Response emission profile, leading to 550 ppmv CO_2 in 2150.

The results for the 550 ppmv CO_2-equivalent pathway imply that there is hardly any scope for flexibility in timing if stabilisation in 2100 is to be achieved without an overshoot, while the 650 ppmv CO_2-equivalents leaves more options open. The profile we constructed in Chapter 3 results in emissions that peak around 2025, but stabilisation can also be reached by earlier or later emission reductions (see Figure 4.3, where the range of emission peaks varies from 2015 to 2035). In other words, stabilising at 550 ppmv CO_2-equivalent without overshoot requires stringent action after 2010 (Kyoto), while stabilisation at 650 ppmv CO_2-equivalent demands less strict mitigation actions after 2010.
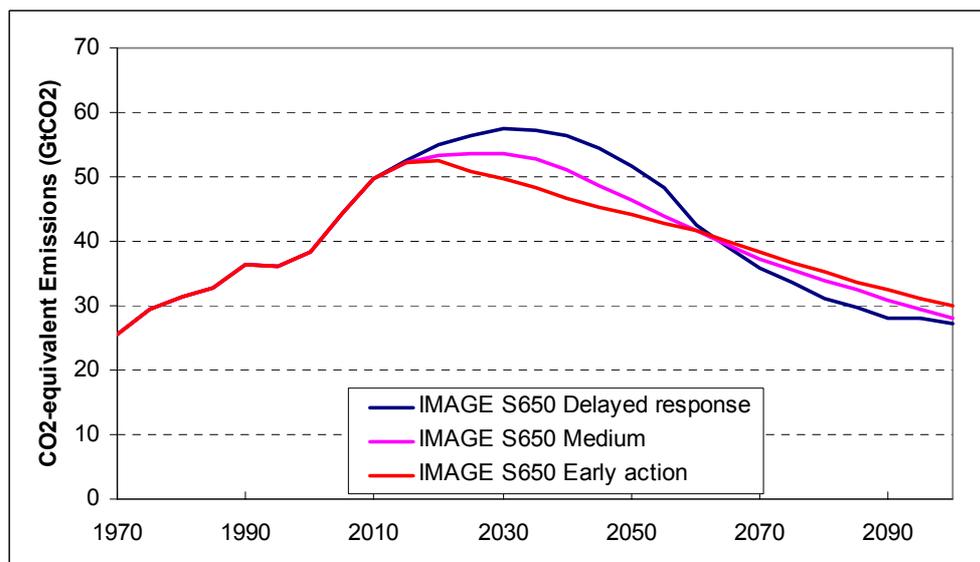
Figure 4.3: Different emission profiles leading to 650 ppmv CO_2-equivalents in 2150. The Medium case is the same profile as shown in Figure 3.4.

4.2 Consequences for the temperature increase

To study whether these constructed profiles stay within the 2°C range (as discussed in the Introduction) we also included assumptions on the sulphur emissions because SO_2 aerosols have a negative impact on radiative forcing. The assumed SO_2 profiles, as discussed in Section 3.6, are shown in Figure 4.4. Logically, the 550 ppmv CO_2-equivalent profile coincides with larger reductions in the SO_2 profile as well.
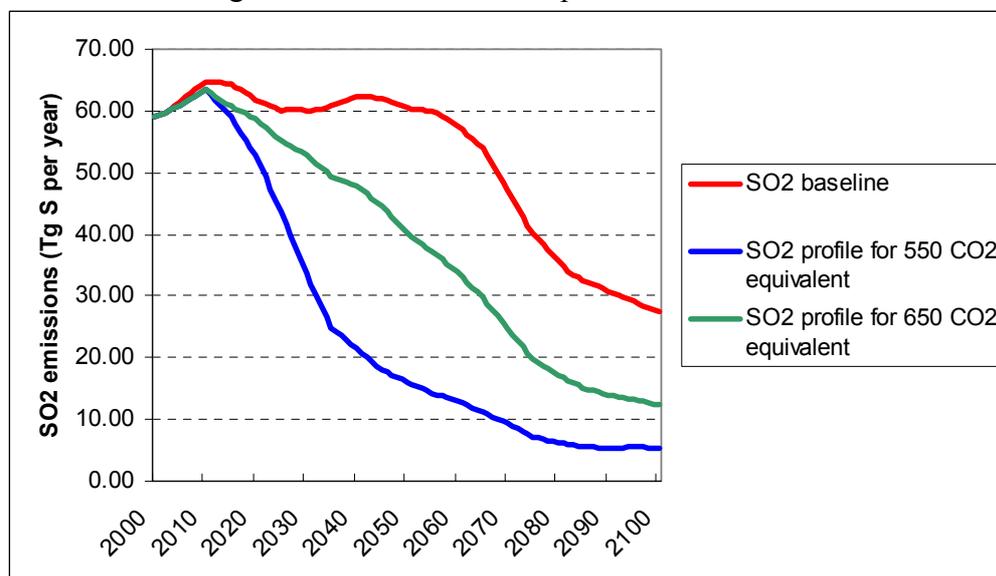

Figure 4.4: SO_2 emission profiles in Tg S per year for the baseline and the two constructed stabilisation profiles.

The resulting global mean surface temperature increases in the baseline and the two constructed stabilisation profiles are plotted in Figure 4.5. For these default cases it is interesting to see that the 550 ppmv CO_2-equivalent profile reaches the 2° Celsius temperature increase above the pre-industrial level in 2100. However, the temperature increase in 2100 is not the equilibrium temperature value because of the inertia in the climate system. In the 650 ppmv CO_2 equivalent stabilisation profile (see Figure 4.5), the

concentration levels have not yet stabilised by 2100 and there will be significant residual warming. The additional warming after 2100 is estimated at 0.4°C (leading to 2.4°C) and 0.6°C (leading to 2.9°C) for the 550 ppmv and 650 ppmv CO_2-equivalents profiles if GHG emissions continu to be reduced after 2100[4]. These estimates are based on the elaboration of the climate sensitivity, but nevertheless, remain highly uncertain because of other factors that influence the final equilibrium temperature increase[5]:

- the behaviour of the biosphere (temperature increase may cause vegetation to become a source instead of a sink; Cox et al., 2000);
- the behaviour of the ocean (temperature increase may cause changes in ocean currents and consequently changes in carbon uptake);
- emissions of aerosols of which some have a warming effect (soot) and others have a cooling effect;
- ozone formation that is dependent of the emissions of ozone precursors like NO_x, CO and non-methane volatile organic compounds (NMVOC).
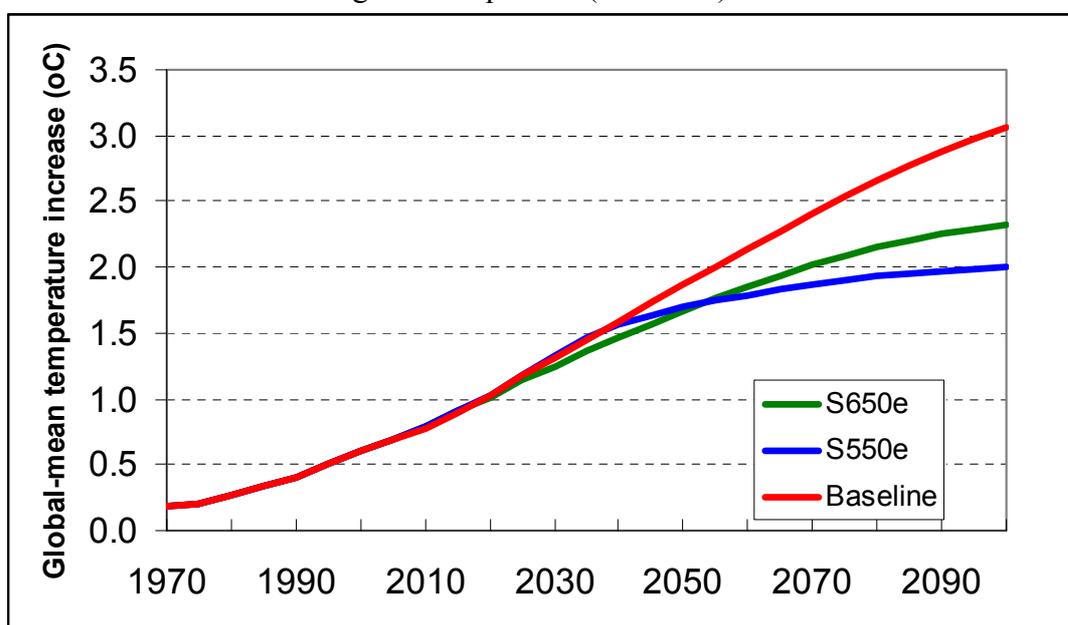

Figure 4.5: Global mean surface temperature increase compared with the pre-industrial level for the baseline and the two constructed stabilisation profiles.

Interestingly, the 550 ppmv CO_2-equivalent profile shows a somewhat higher temperature increase in the period from 2020 to 2050 because of the higher SO_2 emission reductions. This effect is more visible on a graph showing the rate of temperature change (Figure 4.6).

---

[4] IPCC (2001) tends to overestimate the residual temperature increase after stabilisation of CO_2 concentrations because non-CO_2 greenhouse gas emissions follow the A1b path until 2100 and remain constant at the A1b 2100 level thereafter. This assumption is highly debatable given the gap between CO_2 emissions in a 450 ppmv CO_2 stabilisation case and non-CO_2 emissions in the A1b scenario.

[5] Here, we base our estimates on the fact that a doubling of the CO_2 equivalent concentration (from 280 to 560 ppmv) will finally lead to 2.5°C temperature increase. Consequently, an increase to 550 ppmv CO_2-equivalents will lead to 2.4°C (550/560*2.5°C) and an increase to 650 ppmv CO_2-equivalents will lead to 2.9°C (650/560*2.5°C).
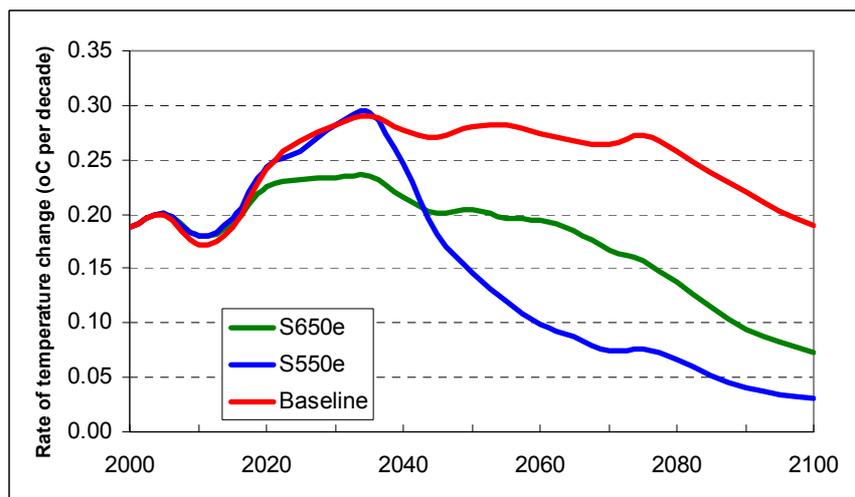
Figure 4.6: Rate of temperature increase for the baseline and the two constructed stabilisation profiles.

Figure 4.6 shows that both stabilisation profiles have a slightly higher rate of temperature increase than the baseline until 2015/2020. The 550 ppmv CO_2-equivalent profile does not fall below the baseline until 2035 and only falls below the 650 ppmv CO_2-equivalent profile around 2045. This shows the dominant effect of SO_2 emissions on the temperature effect in the beginning of the stabilisation profile. Given this reduction in SO_2, emissions, any decrease in temperature resulting from mitigation actions cannot be expected immediately. However, on a local scale regions with presently low levels of SO_2 emissions may already gain from the abatement of GHG emissions on the shorter term.

One final remark can be made on the geographical impact of a global mean temperature effect. Figure 4.7 shows that a 2°C global mean surface temperature increase involves much higher temperature increases above land because of the low temperature effects above oceans. The uncertainty in the climate pattern is high, but Figure 4.7 gives a good indication of the diversity in local temperature effects.
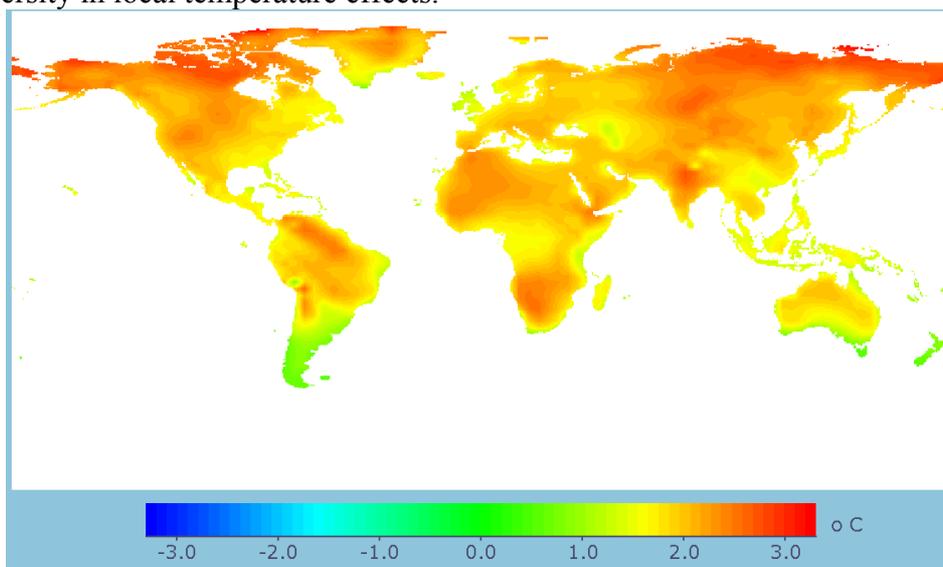

Figure 4.7: Regional distribution of the global mean surface temperature increase of ± 2°C, reached in 2100 by the 550 ppmv CO_2-equivalent profile as shown in Figure 4.9. The regional distribution of the global mean temperature is calculated by using the climate pattern of the HADCM-2 model (Mitchell et al., 1995).

4.3 Emission reduction burden

Figure 4.8 presents the percentage change in *energy- and industry-related* GHG emission levels required under the IMAGE S550e and S650e profiles, compared with the CPI baseline and 1990 levels, for the years 2025, 2050 and 2100. Note that these levels are different from the reductions indicated in Figure 3.4 because of the exclusion of emissions related to land use change. In fact, the reduction in emissions related to land use change in the baseline allow for relatively smaller future reductions in energy- and industry-related greenhouse gases. From Figure 4.8 we can conclude that:

- Stabilisation at both the 550 ppmv and 650 ppmv CO_2-equivalent concentrations requires substantial emission reductions from the CPI baseline, particularly in the long term.
- For the S550e profile, global energy- and industry-related GHG emission levels in 2025 can still increase to about 20% above 1990 levels, but this already implies a substantial emission reduction of 30% compared with baseline levels. For S650e the reduction compared with the baseline is smaller, but still significant at around 15%.
- For stabilisation at 550 ppmv in 2050, emissions have to be reduced strongly, not only compared with the baseline level (approximately 65%) but also compared with 1990 levels (approximately 15%). In contrast, for stabilisation at 650 ppmv the GHG emissions levels may still be 50% above 1990 levels by 2050. However, compared with the baseline, global emissions need to be reduced by about 35%.
- By the end of the century, the stabilisation profiles for both the 550 ppmv and 650 ppmv CO_2-equivalent concentrations imply that global emissions are substantially reduced compared with CPI: by about 70% and 55% respectively. However, when compared with 1990, this implies a reduction of 30% for stabilisation at 550 ppmv CO_2-equivalent and stabilisation at 1990 levels for the 650 ppmv case.
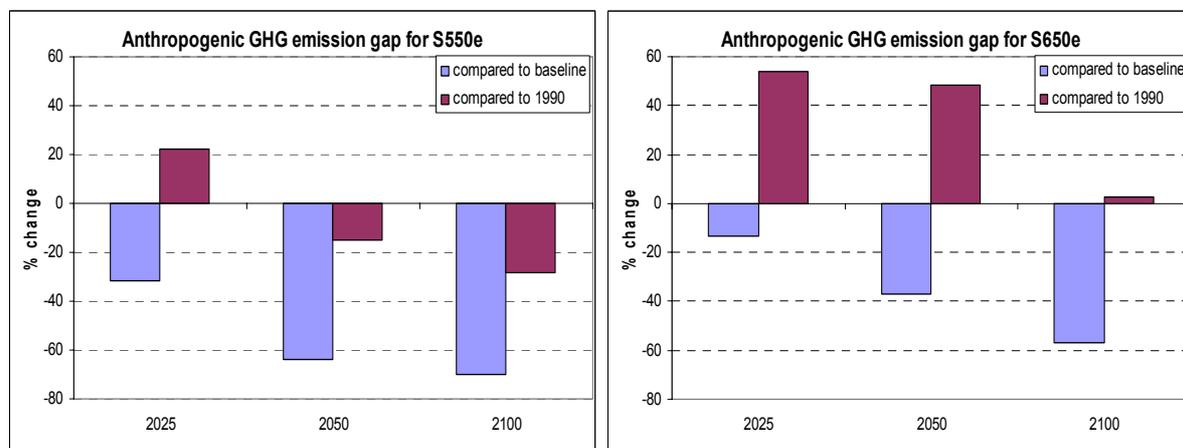

Figure 4.8: Global energy- and industry-related GHG emissions reduction efforts for stabilisation at 550 ppmv (left panel) and 650 ppmv (right panel) CO_2-equivalent levels.

5. Factors important for the temperature increase

The results shown in Chapters 3 and 4 are based on the default settings of the IMAGE 2.2 model and standardised assumptions on the sulphur emissions and share of CO_2 in the CO_2-equivalent profile. In this Chapter we analyse the consequences of changing some sensitive parameters that determine the temperature outcome: the climate sensitivity and SO_2 emissions. The results for changes in these parameters are discussed in Sections 5.1 and 5.2 respectively. In Section 5.3 we analyse whether changes in the share of CO_2 emissions in the equivalent profiles have an impact on the determined CO_2-equivalent concentration and temperature increase. This issue is important when CO_2-equivalent profiles are used for emission reduction strategies based on cost optimisation. This also relates to the discussion on the use of GWPs touched upon in Chapter 2.

5.1 Climate sensitivity
Figure 5.1 shows the results for different climate sensitivity values in the 550 ppmv and 650 ppmv CO_2-equivalent profiles.
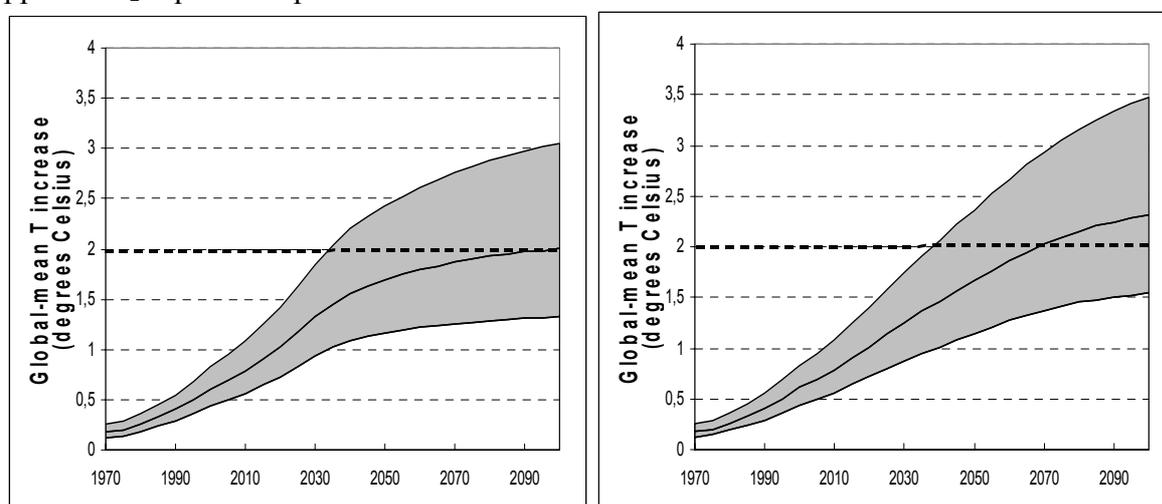

Figure 5.1: Global mean temperature increase since pre-industrial levels resulting from the IMAGE S550e (left panel) and IMAGE S650e (right panel) profiles for different climate sensitivity assumptions (1.5, 2.5 and 4.5). The upper lines indicate the temperature increase resulting from CS=4.5, the middle lines CS=2.5 and the bottom lines CS=1.5; the (horizontal) dotted line is the 2° Celsius target, a climate policy target used by the EU and the Dutch government.

From Figure 5.1 it can be concluded that in principle the IMAGE-550 profile can remain below the maximum global temperature increase of 2°C by 2100 with both medium and low climate sensitivities. The IMAGE-650 profile can only do so with low climate sensitivity, but this profile is likely to overshoot the target by a considerable margin. Neither profile meets the EU target with high climate sensitivity.

This analysis shows the importance of the climate sensitivity when temperature increases are used as targets. IPCC (2001a) has already stated the importance of the climate sensitivity when the temperature increase of the WRE profiles (see Figures 4.1 and 4.2) is calculated with the MAGICC model (Hulme et al., 2000). For this analysis they calibrated the MAGICC model to reproduce the temperature increase of the different General Circulation Models (GCMs). The resulting climate sensitivity ranged from 1.7 to 4.2°C, comparable with the

values used in this study. The calculated temperature increase for the WRE450 profile ranges from 1.2 to 2.3°C and for the WRE550 profile from 1.6 to 2.9°C in the period from 1990 to 2100 (see also Raper et al., 2001). These ranges, mentioned in IPCC (2001a), are also dependent of assumptions on other GHG emissions and sulphur emissions, which the IPCC (2001a) assumed to follow the A1b scenario (Nakicenovic et al., 2000).

5.2 SO_2 emissions

Assumptions about the SO_2 emission profile are also important for the temperature increase because of the cooling effect of sulphate aerosols. The temperature increase for the 550 ppmv and 650 ppmv CO_2-equivalent profiles are shown in Figures 5.2 and 5.3, assuming two different situations regarding the impacts of climate policy on SO_2 emissions: no reductions of SO_2 (baseline) and a reduction in SO_2 emissions proportionate to CO_2 in the same ratio that has been applied so far. The figures show that climate policy, through its effects on SO_2 emissions, not only has an impact on the profile of the temperature effect in the beginning of the mitigation profile, but also has an absolute effect on the level of temperature increase by the end of the century.
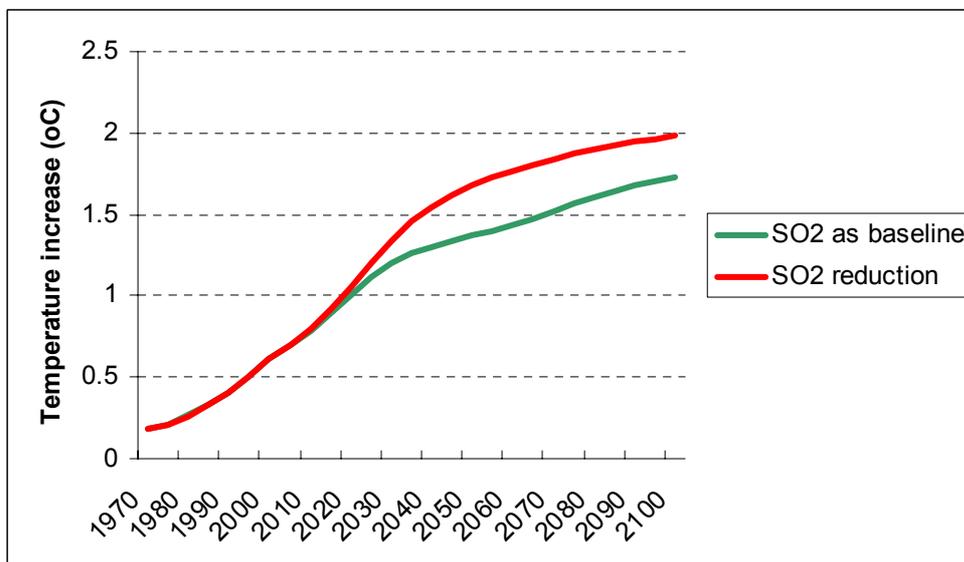

Figure 5.2: Global mean surface temperature increase in the 550 ppmv CO_2-equivalent profile, with SO_2 emissions according to the baseline (green) and SO_2 emission reductions in a fixed ratio to CO_2 emission reductions (red). For SO_2 profiles, see Figure 4.4.

However, since it is reasonable to assume that SO_2 emissions will be further reduced in the longer term, it is fair to say that after 2100 the difference between the temperature profiles will diminish, which can already be seen in Figure 5.2. We can conclude that the uncertainty in climate sensitivity discussed in the previous section has a more important effect on absolute temperature increases after stabilisation than the uncertainty in the sulphur emission profile. This is less true when the rate of temperature increase is used as a climate target (Swart et al., 1998).
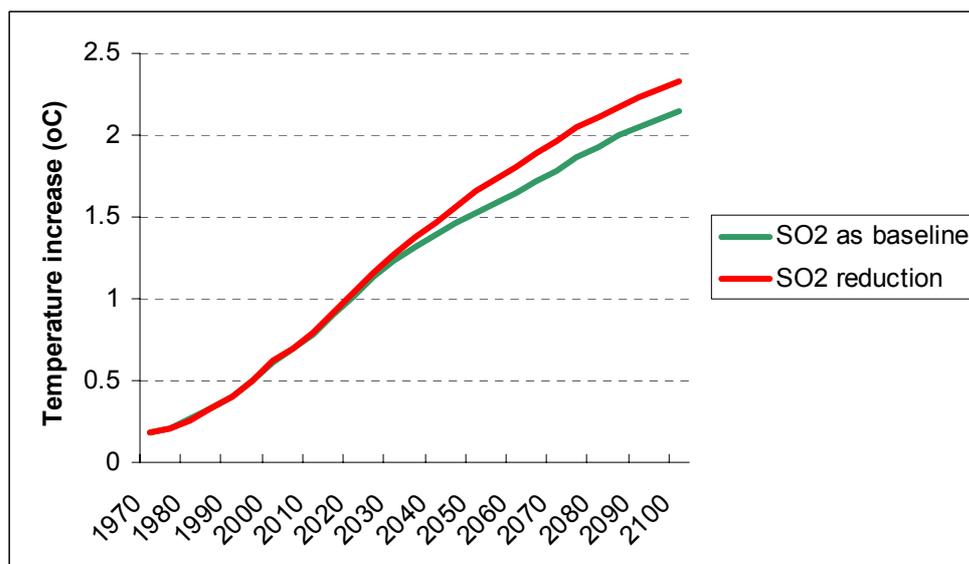
Figure 5.3: Global mean surface temperature increase in the 650 ppmv CO₂-equivalent profile, with SO₂ emissions according the baseline (green) and SO₂ emission reductions in a fixed ratio to CO₂ emission reductions (red). For SO₂ profiles, see Figure 4.4.

5.3 Share of CO₂ and non-CO₂ emissions: use of GWPs

We have developed our GHG stabilisation profiles for use in climate policy and energy models to find the cheapest combination of emission reductions to achieve the CO_2-equivalent emission reductions needed to reproduce the CO_2-equivalent profiles in Figure 3.4. The question is whether researchers can use these CO_2-equivalent profiles (based on GWPs) and substitute freely among different GHGs within the overall emissions given by the profile. This question is important because it is likely that each analysis will result in a different composition of reductions of GHGs than we assumed in the default construction of the IMAGE S550 and IMAGE S650 profiles. To investigate whether changes in the share of CO_2 versus non-CO_2 gases in the overall reduction affect the CO2-equivalent concentration and temperature increases given in Section 4.2, we varied the ratio CO_2 : non-CO_2 in the CO_2-equivalent profiles. Figure 5.4 shows a plot of the share of CO_2 and non-CO_2 over time. The upper panel is the default case. The lower left panel show the situation when non-CO_2 GHGs are assumed to be reduced much more. In this case we assumed 100% reductions in the CH_4 emissions stemming from energy and industry, the sewage system and landfills, and we assumed a 20% reduction in CH_4 emissions from rice fields. For N_2O we assumed 100% emission reductions in the energy system and a 100% reduction in the emissions stemming from industrial activities and the sewage system. Other important land use sources for N_2O, such as fertilisers and animal waste, were assumed to contribute 50% compared with the baseline. All these reduction percentages are reached in 2040. These are clearly ambitious assumptions, but they are meant to give an extreme situation for GHG reductions other than CO_2.
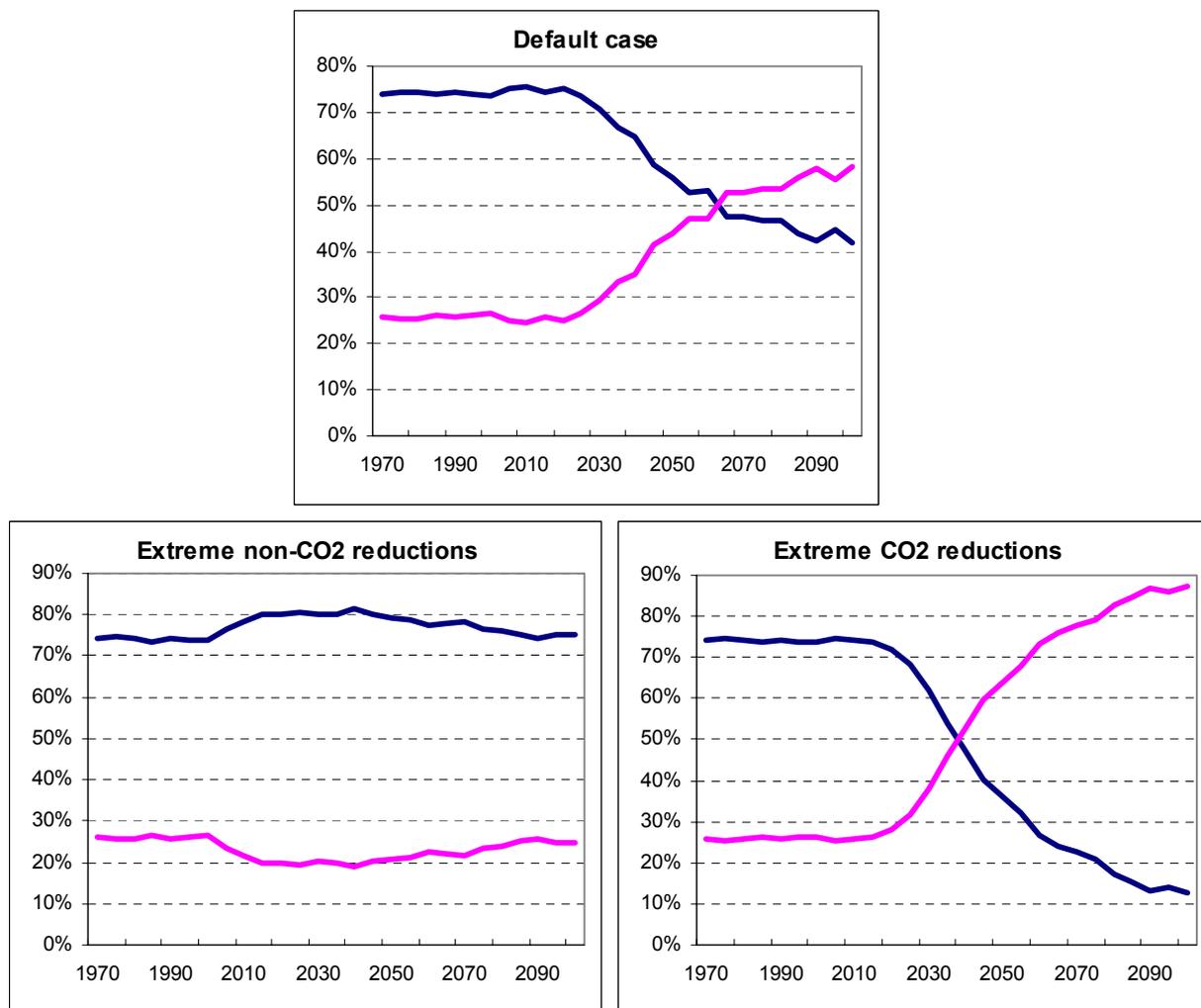
Default case

Extreme non-CO2 reductions

Extreme CO2 reductions

Figure 5.4: Three different cases with a different share in CO_2 (blue) and non-CO_2 greenhouse gases (pink), resulting in similar CO_2-equivalent emission profiles (based on GWP). The upper graph depicts the shares in the default case, leading to 550 ppmv CO_2-equivalents in 2100; below left, with maximum non-CO_2 reductions; below right, with only CO_2 reductions.

In Figure 5.5 we show that equal CO_2-equivalent emission profiles based on GWPs but with different shares of CO_2 and non-CO_2 gases lead to different levels of CO_2-equivalent concentrations (i.e. radiative forcings). When the reductions are only achieved through CO_2 reductions, the CO_2-equivalent concentration reaches a level of 565 ppmv instead of 550 ppmv in the default case. In contrast, the CO_2-equivalent concentration is lower (520 ppmv) when most of the reductions are gained with non-CO_2 gases such as CH_4 and N_2O. An explanation of this result is that the use of a 100 year time horizon for GWPs tends to underestimate the influence of short-lived gases such as CH_4 in the short term (100 years). This means that early steep reductions in non-CO_2 GHGs, as in the case of maximum non-CO_2, lead to more reductions in the radiative forcing than expected from the GWP approach in the period until 2100. The reason for this is that the influence of short-lived gases is spread over 100 years in the GWP approach, while in reality most of the effects occur straight away (in the first 20 years for CH_4). In Figure 5.5 it can be seen that in the case of extreme non-CO_2 reductions the difference from the default case is largest from 2030 to 2060 (when the difference in share of reductions with the default case is most marked, as shown in Figure 5.4). Sygna et al. (2002) have already drawn attention to this problem with the use of GWP,

but also showed that the effect is reversed over the longer term (hundreds of years). Thus, in the extreme case of CO_2-only reductions, the CO_2-equivalent concentration is higher than in the default case for the first 100 years, but lower hundreds of years later. The explanation is that the reduction effect of short-lived gases diminishes and has disappeared entirely after 200 years, while CO_2 reductions continue to have an effect. In Figure 5.5 the difference with the default case is already narrowing in 2100.

These results show that freely substituting reductions of different greenhouse gases on the basis of GWPs leads to substantially different CO_2-equivalent concentration levels in 2100.
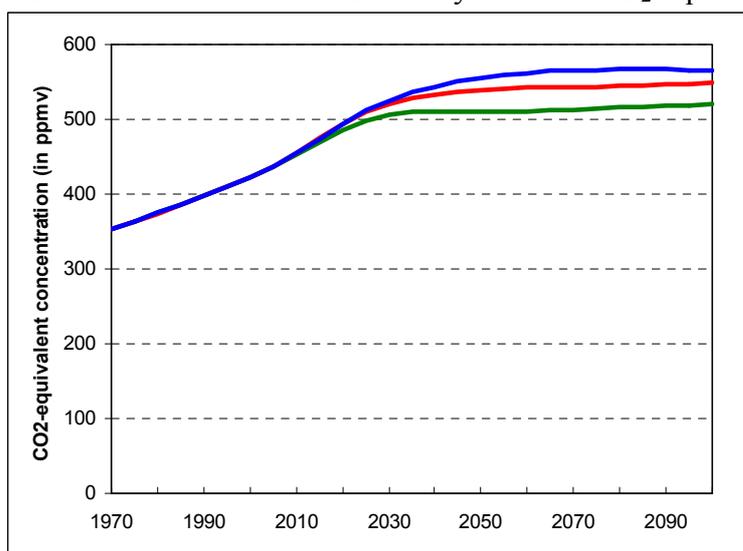
Figure 5.5: Different levels of CO_2-equivalent concentration, resulting from different shares of CO_2 and non-CO_2 emissions, leading to equal CO_2-equivalent emissions (blue = extreme CO_2 reductions; red = default case; green = extreme non-CO_2 reductions).

The resulting temperature effects are shown in Figure 5.6, where the reductions in CO_2-only result in a higher temperature effect than the default case. Although the GWP approach leads to a different temperature effect, the range in temperature increase (~0.5°C) is less than the range in temperature increase due to the uncertainty in the climate sensitivity (~1.6°C).

Figure 5.6: Temperature increase in the different cases shown in Figure 5.4, with the same CO_2-equivalent emission profiles (blue = extreme CO_2 reductions; red = default case; green = extreme non-CO_2 reductions).

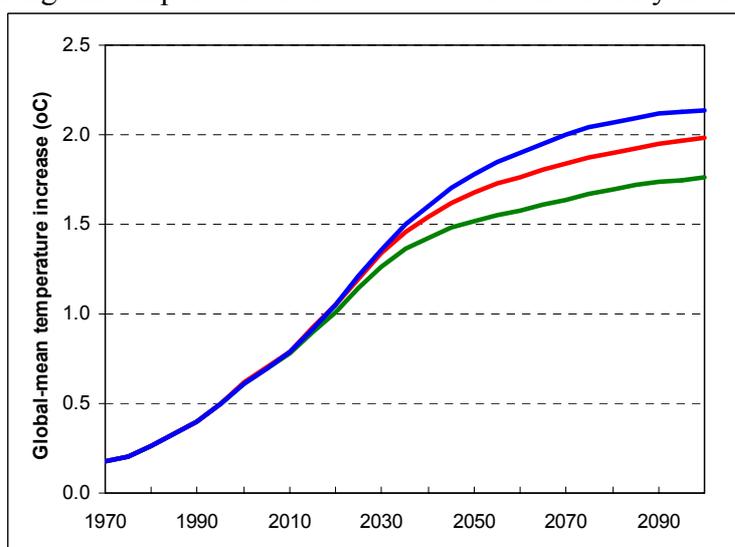Figure 5.7 shows the results for the global mean temperature increase (compared with the pre-industrial age) when the analysis is repeated for the IMAGE S650 profile. The effects on temperature change in Figure 5.7 are similar to the results in Figure 5.6: the range of temperature change is fairly large because of scientific drawbacks of using GWPs. However, the temperature effect has a smaller deviation than the range caused by the different climate sensitivities (Section 5.1).
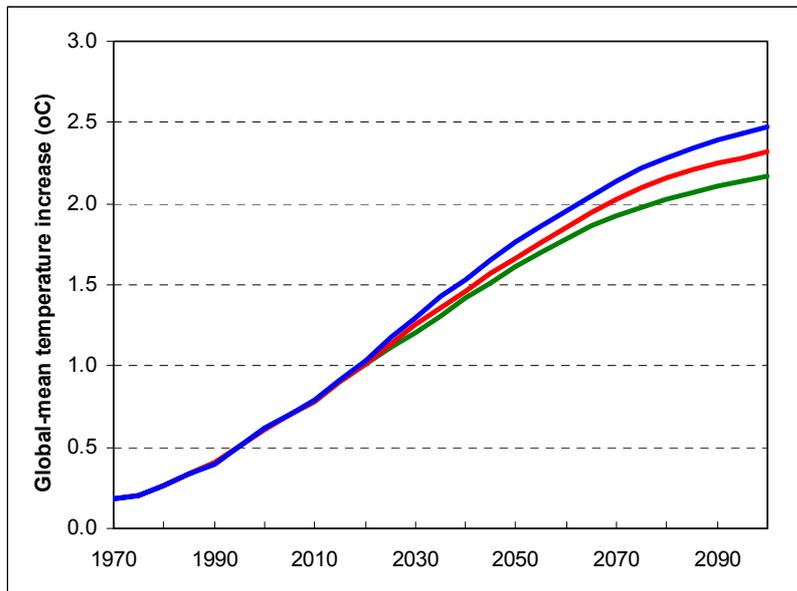

Figure 5.7: Temperature increase with different reduction efforts: the red line represents the default case, leading to 650 ppmv CO_2-equivalents in 2150; the blue line represents the temperature effects when reduction efforts are achieved through CO_2-only; the green line shows the temperature effects in an extreme case of non-CO_2 reductions.

6. Conclusions

In this report we have presented two profiles for total greenhouse gas emissions that lead to stabilisation of GHG concentrations at 550 ppmv and 650 ppmv CO_2-equivalent by 2100 and 2150 respectively. The total greenhouse gas emissions are summed to CO_2 equivalent emissions using the concept of Global Warming Potentials (GWP) and the greenhouse gas concentrations are summed using the total radiative forcing of the Kyoto gases. Until 2010 we implemented the current climate policies as agreed in the Kyoto Protocol and the Bush Climate Initiative. From 2010 to 2100 we used constraints on the maximum reduction rate to account for inertia in the energy system and applied an inverse calculation to determine allowable global emissions to meet the stabilisation levels (without overshoot). From our analyse we conclude that the 550 ppmv profile can result in a maximum global mean temperature increase of less than 2°C, with a low to medium value for the climate sensitivity. The 650 ppmv profile only remains below 2°C if the value for the climate sensitivity is at the low end of the range (from 1.5°C to 4.5°C), which means that this profile is unlikely to meet the target. With a high climate sensitivity of 4.5°C, neither profile meets the 2 °C target. It should be noted that in terms of temperature change, the two profiles only start to diverge from 2050 onwards because of delays within the system and differences in sulphur emission levels.

Stabilising CO_2-equivalent concentrations at 550 ppmv requires substantially larger and earlier global emission reductions than stabilising CO_2-equivalent concentrations at 650 ppmv. The emission profiles leading to a stabilisation of the CO_2-equivalent concentration at 550 ppmv and 650 ppmv peak by 2015 and 2030 respectively. Other possible pathways for reaching the 650 ppmv allow emissions to peak later. For the 550 ppmv CO_2-equivalent a further delay would result in rapid reductions after 2025 (over an emission reduction of 2% per year) and/or a (temporary) overshoot of the 550 ppmv level. The 550 ppmv CO_2 equivalent profile requires a 30% reduction of global GHG emissions in 2050 compared with 1990 levels, which corresponds to a 60% reduction from the baseline we used. In the 650 ppmv CO_2 equivalent profile, 2050 global emissions can be 25% higher than 1990 levels, but this still represents a 35% reduction compared with the baseline.

Our analysis assumed that gases are allocated in such a way that the 550 ppmv and 650 ppmv CO_2-equivalent stabilisation profiles correspond to CO_2 stabilisation at 450 ppmv in 2100 and at 550 ppmv by 2150. These derived CO_2 emission profiles compare well against the WRE profiles used in many IPCC studies.

Moreover, we performed a sensitivity analysis to test the robustness of our findings when we vary our assumptions on sulphur emissions and on the share of CO_2 and non-CO_2 emissions within the CO_2-equivalent profile. Ideally, it would be possible to develop profiles that can be used independently of the baseline from which they are derived and which allow free substitution among the contributors of different forcing agents within the profile, but still result in a similar temperature impact. Unfortunately, our analysis shows that these ideal conditions cannot be met completely. The baseline we used in our analysis has some influence on our results through the emissions from the non-mitigating regions until 2010, through land use emissions and uptake and through the sulphur emissions. From our sensitivity analysis we conclude that the effect on the temperature outcome of different sulphur mitigation efforts is small compared with the effect of different values for the climate sensitivity.

Our analysis also shows that different compositions of GHGs within the CO_2-equivalent emission profiles lead to other CO_2-equivalent concentrations (i.e. radiative forcing) and temperature impacts. This result shows the limitations inherent in the use of GWPs for temperature targets. With the common 100 year time horizon the effect of reduction efforts for short-lived gases such as CH_4 is underestimated in the first 40 years. On the other hand, the temperature effects of measures to reduce CO_2 are underestimated over the long term (over 100 years). Taking other disadvantages of the GWP concept into account, such as not being able to include all climate-forcing agents (e.g. aerosols) in the analysis, we suggest that more research should to be conducted to find appropriate alternatives to the GWP concept in multi-gas analyses.

References

Alcamo, J., Kreileman, G.J.J., Krol, M.S., Leemans, R., Bollen, J.C., Van Minnen, J.G., Schaeffer, M., Toet, A.M.C. and De Vries, H.J.M., 1998. Global modelling of environmental change: an overview of IMAGE 2.1. In: Alcamo, J., Leemans, R. and Kreileman, G.J.J. (Eds.), Global change scenarios of the 21st century. Results from the IMAGE 2.1 model. Elsevier Science, London, United Kingdom, pp. 3-94.

Berk, M.M., and Den Elzen, M.G.J., 2001. Options for differentiation of future commitments in climate policy: how to realise timely participation to meet stringent climate goals. Climate Policy, 1: 465-480.

Berk, M.M., Van Minnen, J.G., Metz, B., and Moomaw, W., 2001. Keeping our options open. A strategic Vision on Near-term Implications of Long-term Climate Policy Options. Results from the COOL project. National Institute for Public Health and the Environment, Bilthoven, the Netherlands.

Cox, P. M., Betts, R. A. and Jones, C. D., 2000. Acceleration of global warming due to carbon-cycle feedbacks in a coupled climate model. Nature, 408: 180-184.

Criqui, P. and Kouvaritakis, N., 2000. World energy projections to 2030. International Journal of Global Energy Issues, 14(1, 2, 3, 4): 116-136.

De Jager, D., Hendriks, C.A., Byers, C., Van Brummelen, M., Petersdorff, C., Struker, A.H.M., Blok, K., Oonk, J., Gerbens, S. and Zeeman., G., 2001. Emission reduction of non-CO_2 greenhouse gases. NRP-report 410200094, Dutch National Research Programme on Global Air Pollution and Climate Change, Bilthoven, the Netherlands.

De Vries, H.J.M., Van Vuuren, D.P., Den Elzen, M.G.J. and Janssen, M.A., 2001. The Targets IMage Energy Regional (TIMER) Model. Technical Documentation. RIVM-report 461502024, National Institute for Public Health and the Environment, Bilthoven, the Netherlands.

Den Elzen, M.G.J., and De Moor, A.P.G., 2002. Evaluating the Bonn-Marrakech agreement. Research letter. Climate Policy, **2**, 111-117.

Den Elzen, M.G.J., and Lucas, P., 2003. FAIR 2.0 - A decision-support tool to assess the environmental and economic consequences of future climate regimes. RIVM report 550015001, National Institute for Public Health and the Environment, Bilthoven, the Netherlands.

Eickhout, B., Den Elzen, M.G.J. and Kreileman, G.J.J., 2003. The atmosphere-ocean system of IMAGE 2.2. A global model approach for atmospheric concentrations and climate and sea level projections. RIVM-report 481508017, National Institute for Public Health and the Environment, Bilthoven, the Netherlands. (in prep.)

Enting, I.G., Wigley, T.M.L. and Heimann, M., 1994. Future Emissions and Concentrations of Carbon Dioxide: Key Ocean/Atmosphere/Land Analyses. CSIRO Technical Paper No. 31, Co-operative Research Centre for Southern Hemisphere Meteorology, Division of Atmospheric Research, Australia.

Fuglestvedt, J.S., Berntsen, T.K., Godal, O., Sausen, R., Shine, K.P. and Skodvin, T., 2003. Metrics of climate change: Assessing radiative forcing and emission indices. Climatic Change, 58: 267-331.

Hansen, J., Sato, M., Ruedy, R., Lacis, A., and Oinas, V., 2000. Global warming in the twenty-first century: An alternative scenario. Proc. Natl. Acad. Sci., 97, 9875-9880.

Harvey, D., Gregory, J., Hoffert, M., Jain, A., Lal, M., Leemans, R., Raper, S., Wigley, T. and De Wolde, J., 1997. An introduction to simple climate models used in the IPCC second assessment report. IPCC Technical Paper II, Geneva, Switzerland.

Hulme, M., Wigley, T., Barrow, E., Raper, S., Centella, A., Smith, S. and Chipanski, A., 2000. Using a climate scenario generator for vulnerability and adaptation assessments: MAGICC and SCENGEN version 2.4 workbook. Norwich, United Kingdom.

IMAGE team, 2001. The IMAGE 2.2 implementation of the SRES scenarios. A comprehensive analysis of emissions, climate change and impacts in the 21st century. CD-ROM publication 481508018, National Institute for Public Health and the Environment, Bilthoven, the Netherlands.

IPCC, 1990. Climate Change. The Scientific Assessment. UNEP/WMO. Cambridge University Press, Cambridge, United Kingdom.

IPCC, 1994. Climate Change 1994. Radiative Forcing of Climate Change and an Evaluation of the IPCC IS92 Emission Scenarios. [Eds. Houghton, J.T., Meira Filho, L.G., Bruce, J., Lee, H., Callander, B.A., Haites, E., Harris, N. and Maskell, K.]. Cambridge University Press, Cambridge, United Kingdom.

IPCC, 2001a. Climate Change 2001: the Scientific Basis. Contribution of Working Group I to the Third Assessment Report of the Intergovernmental Panel on Climate Change [Eds. Houghton, J.T., Ding, Y., Griggs, D.J., Noguer, M., Van der Linden, P.J., Dai, X., Maskell, K. and Johnson, C.A.]. Cambridge University Press, Cambridge, United Kingdom and New York, NY, U.S.A.

IPCC, 2001b. Climate Change 2001: Impacts, Adaptation and Vulnerability. Contribution of Working Group II to the Third Assessment Report of the Intergovernmental Panel on Climate Change [Eds. McCarthy, J.J., Canziani, O.F., Leary, N.A., Dokken, D.J. and White, K.S.]. Cambridge University Press, Cambridge, United Kingdom and New York, NY, U.S.A.

IPCC, 2001c. Climate Change 2001: Mitigation. Contribution of Working Group III to the Third Assessment Report of the Intergovernmental Panel on Climate Change [Eds. Metz, B., Davidson, O., Swart, R. and Pan, J.]. Cambridge University Press, Cambridge, United Kingdom and New York, NY, U.S.A.

IPCC, 2001d. Climate Change 2001: Synthesis Report. Contribution of Working Groups I, II, and III to the Third Assessment Report of the Intergovernmental Panel on Climate Change [Eds. Watson, R.T. and the Core Writing Team]. Cambridge University Press, Cambridge, United Kingdom and New York, NY, U.S.A.

Manne, A.S. and Richels, R.G., 2001. An alternative approach to establishing trade-offs among greenhouse gases. Nature, 410: 675-677.

Mitchell, J.F.B., Johns, T.C., Gregory, J.M. and Tett, S.F.B., 1995. Climate response to increasing levels of greenhouse gases and sulphate aerosols. Nature, 376, 501-504.

Morita, T., Nakicenovic, N., and Robinson, J., 2000. Overview of Mitigation Scenarios for Global Climate Stabilisation based on New IPCC Emission Scenarios (SRES). Environmental Economics and Policy Studies, 3(2).

Nakicenovic et al., 2000. Special Report on Emissions Scenarios. A Special Report of Working Group III of the Intergovernmental Panel on Climate Change. Cambridge University Press, Cambridge, United Kingdom, New York, NY, U.S.A., Melbourne, Australia and Madrid, Spain, 599 pp.

O'Neill, B.C., 2003. Economics, Natural Science, and the Costs of Global Warming Potentials. Climatic Change, 58: 251-260.

O'Neill, B.C., and Oppenheimer, M., 2002. Dangerous Climate Impacts and the Kyoto Protocol. Science, 296, 1971-1972.

Raper, S.C.B., Gregory, J.M., and Osborn, T.J., 2001. Use of an upwelling-diffusion energy balance climate model to simulate and diagnose A/OGCM results. Climate Dynamics, 17, 601-613.

Rayner, S., and E. Malone (Eds.), 1998. Human Choice and Climate Change. Battelle Press, Columbus, Ohio, USA.

Reilly, J.M. et al.: 1999. Multi-Gas Assessment of the Kyoto Protocol. Nature, 401: 549-555.

Smith, S.J., 2003. The Evaluation of Greenhouse Gas Indices. Climatic Change, 58: 261-265.

Smith, S.J. and Wigley, T.M.L., 2000a. Global Warming Potentials: 1. Climatic implications of emission reductions. Climatic Change, 44: 445-457.

Smith, S.J. and Wigley, T.M.L., 2000b. Global Warming Potentials: 2. Accuracy. Climatic Change, 44: 459-469.

Swart, R., Berk, M.M., Janssen, M., Kreileman, G.J.J. and Leemans, R., 1998. The safe landing analysis: risks and trade-offs in climate change. In: Global change scenarios of the 21st century. Results from the IMAGE 2.1 model. (Eds. Alcamo, J., Leemans, R. and Kreileman, G.J.J.), Elseviers Science, London. pp. 193-218.

Sygna, L., Fuglestvedt, J.S. and Aaheim, H.A., 2002. The Adequacy of GWPs as indicators of damage costs incurred by global warming. Mitigation and Adaptation Strategies for Global Change, **7**: 45-63.

Van Minnen, J.G., Leemans, R. and Ihle, F., 2000. Defining the importance of including transient ecosystem responses to simulate C-cycle dynamics in a global change model. Global Change Biology, 6: 595-611.

Van Vuuren, D.P. and De Vries, H.J.M., 2001. Mitigation scenarios in a world oriented at sustainable development: the role of technology efficiency and timing. Climate Policy, 1: 189-210.

Van Vuuren, D.P., Den Elzen, M.G.J., Berk, M.M., Lucas, P., Eickhout, B., Eerens, H. and Oostenrijk, R., 2003. Regional costs and benefits of alternative post-Kyoto climate regimes. Comparison of variants of the Multi-stage and Per Capita Convergence regimes. RIVM report 728001025, National Institute for Public Health and the Environment, Bilthoven, the Netherlands.

Wigley, T.M.L., Richels, R. and Edmands, J.A., 1996. Economic and environmental choices
    in the stabilisation of atmospheric CO_2 concentrations. Nature, 379: 240-243.

Appendix A: Calculating GWPs and radiative forcings

Equivalent emissions
The CO_2-equivalent emissions (in Tg CO_2 per year) are computed according to the following simple equation:

$$E_{CO_2-eq} = E_{GHG} \cdot GWP \qquad\qquad (A.1)$$

with GWP being the Global Warming Potential (in Tg CO_2 per Tg GHG) and E_{GHG} the annual emission of the greenhouse gas (in Tg GHG per year) taken into account (CO_2, CH_4, N_2O, the HFCs, PFCs and SF_6). The direct GWP is relative to carbon dioxide for a 100-year time horizon. We used the estimates from IPCC (2001a). For example, the GWP for CH_4 is 23, which means that 1 kg of CH_4 has the same impact as 23 kg of CO_2 for a time horizon of 100 years. The GWP for N_2O is 296. GWPs for the other substances cover a wide range of values up to 22,200 for SF_6 (IPCC, 2001).

Equivalent concentrations
For the calculation of the equivalent concentrations we used the direct relation of each gas to its radiative forcing. From the sum of all radiative forcings we can calculate the CO_2-equivalent concentration. We mainly used the Special Report on Simple Climate Models (Harvey et al., 1997) and the Contribution of Working Group I to the TAR (IPCC, 2001a) to calculate the radiative forcing of each Kyoto gas from its atmospheric concentration (see also Eickhout et al., 2003).

The radiative forcing of carbon dioxide is calculated as follows:

$$\Delta Q_{CO_2,t} = 5.325 \cdot \ln\left(\frac{[CO_2]_t}{[CO_2]_{t_0}}\right) \qquad\qquad (A.2)$$

where t_0 is the pre-industrial age (1765, the year of initialisation in IMAGE 2.2). The pre-industrial concentration of CO_2 is assumed to be 278 ppmv. The value 5.325 stems from the fact that a doubling of the CO_2 concentration since pre-industrial times will lead to an increased forcing of 3.7 Wm^{-2}. This is in line with the assumed value of IPCC (2001).

For CH_4 and N_2O we have to consider that as the concentration of these greenhouse gases increases, the dependence of each forcing on both concentrations will gradually 'saturate', since both gases absorb in each other's frequency domains. To take this mechanism into account, IMAGE 2.2 uses the following equations (IPCC, 2001):

$$
\begin{aligned}
\Delta Q_{CH_4,t} = {} & 0.036 \cdot \left(\sqrt{[CH_4]_t} - \sqrt{[CH_4]_{t_0}}\right) - \\
& \left(
\begin{aligned}
& 0.47 \cdot \ln\left[\begin{array}{l} 1 + a \cdot \left([CH_4]_t \cdot [N_2O]_{t_0}\right)^{0.75} + \\ b \cdot [CH_4]_t \left([CH_4]_t \cdot [N_2O]_{t_0}\right)^{1.52} \end{array}\right] - \\
& 0.47 \cdot \ln\left[\begin{array}{l} 1 + a \cdot \left([CH_4]_{t_0} \cdot [N_2O]_{t_0}\right)^{0.75} + \\ b \cdot [CH_4]_{t_0} \left([CH_4]_{t_0} \cdot [N_2O]_{t_0}\right)^{1.52} \end{array}\right]
\end{aligned}
\right)
\end{aligned}
\qquad (A.3)
$$

for the change in radiative forcing of methane, and:

$$\Delta Q_{N_2O,t} = 0.12 \cdot \left(\sqrt{[N_2O]_t} - \sqrt{[N_2O]_{t_0}} \right) -$$
$$\left(0.47 \cdot \ln \left[\begin{array}{c} 1 + a \cdot \left([CH_4]_{t_0} \cdot [N_2O]_t \right)^{0.75} + \\ b \cdot [CH_4]_{t_0} \left([CH_4]_{t_0} \cdot [N_2O]_t \right)^{1.52} \end{array} \right] - \right.$$
$$\left. 0.47 \cdot \ln \left[\begin{array}{c} 1 + a \cdot \left([CH_4]_{t_0} \cdot [N_2O]_{t_0} \right)^{0.75} + \\ b \cdot [CH_4]_{t_0} \left([CH_4]_{t_0} \cdot [N_2O]_{t_0} \right)^{1.52} \end{array} \right] \right) \qquad (A.4)$$

for the change in radiative forcing of nitrous oxide. The pre-industrial concentrations $[CH_4]_{t_0}$ and $[N_2O]_{t_0}$ are assumed to be 700 ppbv and 270 ppbv respectively (IPCC, 2001). The values a and b are 2.01 x 10^{-5} and 5.31 x 10^{-15}.

For the HFCs, PFCs and SF_6 the radiative forcing is calculated by multiplying the tropospheric concentrations by the 'radiative efficiency coefficients' taken from IPCC (2001). Table A.1 contains the radiative efficiency coefficients used in IMAGE 2.2.

Table A.1: Radiative efficiency coefficients of the HFCs, PFCs and SF_6 taken into account by IMAGE 2.2, based on IPCC (2001).

Chemical compound	Radiative efficiency coefficient (in $W*m^{-2}*ppbv^{-1}$)
HFC-23	0.16
HFC-32	0.09
HFC-43-10-mee	0.40
HFC-125	0.23
HFC-134a	0.15
HFC-143a	0.13
HFC-152a	0.09
HFC-227ea	0.30
HFC-236fa	0.28
HFC-245ca	0.23
CF_4 [1]	0.08
C_2F_6	0.26
SF_6	0.52

1) *The pre-industrial concentration of naturally occurring GHGs is subtracted before multiplying by the radiative efficiency coefficient to obtain the radiative forcing compared with pre-industrial times. Of these gases only CF_4 occurs naturally, at an assumed level of 40 ppbv.*

After summing these different radiative forcings, the CO_2-equivalent concentration is calculated by an inverse equation of Equation A.2 (see Equation A.5),

$$[CO_2 - equivalent]_t = [CO_2]_{t_0} \cdot e^{\frac{\sum \Delta Q_{GHG,t}}{5.325}} \qquad (A.5)$$

where the pre-industrial concentration is again assumed to be 278 ppmv.

Appendix B: Elaboration on Padé approximant

The visualisation of the Padé approximant described in Section 3.4 (see here Equation B.1) leads to a curve that resembles a stabilisation profile of atmospheric CO_2 concentration. For this reason this mathematical approximant was introduced as a stabilisation profile by Enting et al. (1994). Any desired stabilisation profile can be determined by defining 5 constraints to the approximant. This Appendix contains the algebra for calculating the values a, b, c, d and e in Equation B.1 by defining the 5 constraints, subsequently leading to a stabilisation profile.

$$f(x) = \frac{a + bx + cx^2}{1 + dx + ex^2} \qquad\qquad (B.1)$$
with: $0 \le x \le 1$

The five constraints explained in Section 3.4 are the following:
1. $h(0) = r$
2. $h'(0) = q$
3. $h(1) = p$ $\qquad\qquad (B.2)$
4. $h'(1) = 0$
5. $h(x_t) = s$

First, we assume function $h(x)$ without value a. The derivative of function h is:

$$h'(x) = \frac{(b + 2cx)(1 + dx + ex^2) - (d + 2ex)(bx + cx^2)}{(1 + dx + ex^2)^2} \qquad\qquad (B.3)$$

The first two constraints from Equation B.2 lead to the following definitions:
1. $r = 0$ $\qquad\qquad (B.4)$
2. $q = b$

The other three constraints are elaborated as follows:

3. $p = \dfrac{b + c}{1 + d + e}$

4. $b(1 - e) + c(d + 2) = 0$ $\qquad\qquad (B.5)$

5. $s = \dfrac{bx_t + cx_t^2}{1 + dx_t + ex_t^2}$

Combination of 3 and 4 in B.5 leads to the following cascade of equations:

$b(1-e)$	$+ \quad c(d+2)$	$=$	0	4.
b	$+ \quad c$	$=$	$p(1+d+e)$	3.
$b(1-e)$	$+ \quad c(1-e)$	$=$	$p(1+d+e)(1-e)$ $\;\leftrightarrow\;$	3.*$(1-e)$
0	$+ \quad c(1+d+e)$	$=$	$p(e-1)(1+d+e)$	4.$-$3.*$(1-e)$

In other words:
$$c = p(e-1) \quad \wedge \quad (1 + d + e) \ne 0 \qquad\qquad (B.6)$$

The combination of the fourth constraint and the Equations B.4 and B.6 leads to:

$$d = \frac{q}{p} - 2 \qquad\qquad (B.7)$$

So far, the elaboration has given more insight into the values *a*, *b* and *d*. The values *c* and *e* still have unknown variables in the definitions. The fifth constraint is needed to resolve this issue. Elaboration on the fifth constraint in Equation B.5, by substituting the variables *b*, *c* and *d* with Equations B.4, B.6 and B.7, returns the following equation for *e*:

$$e = \frac{1}{(s-p)x_t^2}\left[qx_t - px_t^2 - s\left(1 + \frac{q}{p}x_t - 2x_t\right)\right] \tag{B.8}$$

Now, value *c* can be written as a defined value as well:

$$c = \frac{p}{(s-p)x_t^2}\left[qx_t - s\left(x_t^2 + 1 + \frac{q}{p}x_t - 2x_t\right)\right] \tag{B.9}$$

The previous elaboration has returned known values for the 5 unknown values in the Padé approximant, using the 5 constraints given a priori. However, so far the function *h* has been elaborated with value *a* equals 0. Function *f* is the Padé approximant needed for the stabilisation profile. Hence, the value *a* is added to the previous elaboration, returning the following 5 definitions of the 5 unknown variables in the Padé approximant from equation B.1:

$$a = r$$

$$d = \frac{q}{p-a} - 2$$

$$b = a \cdot d + q \tag{B.10}$$

$$e = \frac{1}{(s-p)x_t^2}\left[qx_t - (p-a)x_t^2 - (s-a)(1 + dx_t)\right]$$

$$c = \frac{p-a}{(s-p)x_t^2}\left[qx_t - (s-a)(x_t^2 + 1 + dx_t)\right] + ae$$

Thus, by defining 5 constraints as summed in Equation B.2, the values *a*, *b*, *c*, *d* and *e* can be calculated according Equation B.10, leading to any desired stabilisation profile.